LOAN DOCUMENT

PHOTOGRAPH THIS SHEET

DTIC ACCESSION NUMBER

LEVEL

INVENTORY

AL/EQ-TR-1997-0022

DOCUMENT IDENTIFICATION

1 May 97

DISTRIBUTION STATEMENT A

Approved for public release:
Distribution Unlimited

DISTRIBUTION STATEMENT

H A N D L E

ACCESSION FOR

NTIS	GRAAI	☑
DTIC	TRAC	☐
UNANNOUNCED		☐
JUSTIFICATION		

BY

DISTRIBUTION/

AVAILABILITY CODES

| DISTRIBUTION | AVAILABILITY AND/OR SPECIAL |
| A-1 | |

DISTRIBUTION STAMP

DATE ACCESSIONED

DTIC QUALITY INSPECTED 1

DATE RETURNED

19980904 008

DATE RECEIVED IN DTIC

REGISTERED OR CERTIFIED NUMBER

W I T H

C A R E

PHOTOGRAPH THIS SHEET AND RETURN TO DTIC-FDAC

DOCUMENT PROCESSING SHEET

PREVIOUS EDITIONS MAY BE USED UNTIL
STOCK IS EXHAUSTED.

LOAN DOCUMENT

Environmental Security
Technology Certification
Program

AL/EQ-TR-1997-0022

EVALUATION OF PILOT-SCALE PULSE-CORONA-INDUCED PLASMA DEVICE TO REMOVE NOx FROM COMBUSTION EXHAUSTS FROM A SUBSCALE COMBUSTOR AND FROM A HUSH HOUSE AT NELLIS AFB, NEVADA

SHEILA M. HAYTHORNTHWAITE, MICHAEL D. DURHAM,
GARY L. ANDERSON, AND DONALD E. RUGG
ADA TECHNOLOGIES, INC.
304 INVERNESS WAY SOUTH, SUITE 365
ENGLEWOOD, CO 80112

1 MAY 1997

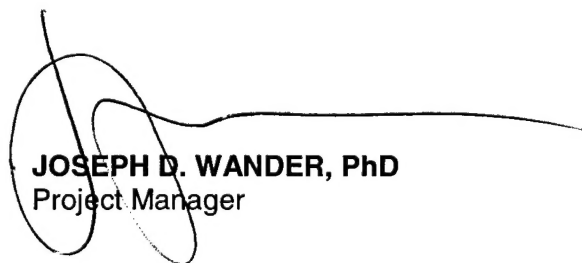FINAL REPORT: AUGUST 1994 – JANUARY 1997

NOTICES

This report was prepared as an account of work sponsored by an agency of the United States Government. Neither the United States Government nor any agency thereof, nor any employees, nor their contractors, subcontractors, or their employees make any warranty, express or implied, or assume any legal liability or responsibility for the accuracy, completeness, or usefulness of any privately owned rights. References herein to any specific commercial process or service by trade name, trademark, manufacturer, or otherwise does not necessarily constitute or imply its endorsement, recommendation, or favoring by the United States Government or any agency, contractor, or subcontractor thereof. The views and opinions of the authors expressed herein do not necessarily state or reflect those of the United States Government or of any agency, contractor, or subcontractor thereof.

When government drawings, specifications, or other data are used for any purpose other than in connection with a definitely government-related procurement, United States Government incurs no responsibility or obligations, whatsoever. The fact that the Government may have formulated or in any way supplied the said drawings, specifications or other data is not to be regarded by implication, or otherwise in any other manner construed, as licensing the holder or any other person or corporation, or as conveying any rights or permission to manufacture, use or sell any patented invention that may in any way be related thereto.

This is an SBIR Phase II report. The contractor has given permission for public release. This technical report has been reviewed by the Public Affairs Office [PA] and is releasable to the National Technical Information Service, where it will be available to the general public, including foreign nations.

This report has been reviewed and is approved for publication.

JOSEPH D. WANDER, PhD
Project Manager

CHRISTINE WAGENER-HULME, Lt Col, USAF, BSC
Chief, Environmental Technology
Development Branch

If your address has changed, if you wish to be removed from our distribution list, or if the addressee is no longer employed by your organization, please notify AFRL/MLQP, Tyndall AFB, Florida 32403-5323, or andrew.poulis@ccmail.aleq.tyndall.af.mil.

Do not return copies of this report unless contractual obligations or notice on a specific document requires its return.

REPORT DOCUMENTATION PAGE

Public reporting burden for this collection of information is estimated to average 1 hour per response, including the time for reviewing instructions, searching existing data sources, gathering and maintaining the data needed, and completing and reviewing the collection of information. Send comments regarding this burden estimate or any other aspect of this collection of information, including suggestions for reducing this burden, to Washington Headquarters Services, Directorate for Information Operations and Reports, 1215 Jefferson Davis Highway, Suite 1204, Arlington, VA 22202-4302, and to the Office of Management and Budget, Paperwork Reduction Project (0704-0188), Washington, DC 20503.

1. AGENCY USE ONLY (Leave blank)	2. REPORT DATE	3. REPORT TYPE AND DATES COVERED
	970501	Final, 9408--9701

4. TITLE AND SUBTITLE
Evaluation of a Pilot-Scale Pulse-Corona-Induced Plasma Device to Remove NOx from Combustion Exhausts from a Subscale Combustor and from a Hush House at Nellis AFB, Nevada

5. FUNDING NUMBERS
Contract No. F08637-94-C-6047
JON: 2103 S403

supplement:
USN AESO MIPR
N0001994WXC8KFL

6. AUTHOR(S)
Sheila M. Haythornthwaite, Michael D. Durham, Gary L. Anderson, and Donald E. Rugg

7. PERFORMING ORGANIZATION NAME(S) AND ADDRESS(ES)
ADA Technologies, Inc.
304 Inverness Way South, Suite 365
Englewood, CO 80112

8. PERFORMING ORGANIZATION REPORT NUMBER
R439198F01

9. SPONSORING/MONITORING AGENCY NAME(S) AND ADDRESS(ES)
AL/EQM
139 Barnes Drive, Suite 2
Tyndall AFB, FL 32403-5323

10. SPONSORING/MONITORING AGENCY REPORT NUMBER
AL/EQ-TR-1997-0022

11. SUPPLEMENTARY NOTES
Technical Monitor: Dr Joe Wander, AFRL/MLQ, DSN 523-6240,
COMM (850) 283-6240

12a. DISTRIBUTION AVAILABILITY STATEMENT
Approved for Public Release; Distribution Unlimited

12b. DISTRIBUTION CODE
A

13. ABSTRACT (Maximum 200 words)
Jet engine test cells (JETCs) are used to test-fire new, installed, and reworked jet engines. Because JETCs have been classified as stationary sources of pollutant emissions, they are subject to possible regulation under Title I of the Clean Air Act (CAA) as amended in 1990. In Phase I of the Small Business Innovation Research (SBIR) program, a novel NOx-control approach utilizing pulsed-corona-induced plasma successfully showed 90% removal of NOx in the laboratory. The objective of Phase II was to reproduce the laboratory-scale results in a pilot-scale system. The technology was successfully demonstrated at pilot scale in the field, on a slipstream of JETC flue gas at Nellis Air Force Base. Based on the field data, cost projections were made for a system to treat the full JETC exhaust. The technology efficiently converted NO into ONO, and a wet scrubber was required to achieve the treatment goal of 50-percent removal and destruction of NOx. The plasma simultaneously removes hydrocarbons from the flue gas stream. This project demonstrated that pulse-corona-induced plasma technology is scalable to practical industrial dimensions.

14. SUBJECT TERMS
NOx control, corona discharge, test cells, nonthermal discharge, plasma discharge

15. NUMBER OF PAGES
84

16. PRICE CODE

17. SECURITY CLASSIFICATION OF REPORT	18. SECURITY CLASSIFICATION OF THIS PAGE	19. SECURITY CLASSIFICATION OF ABSTRACT	20. LIMITATION OF ABSTRACT
Unclassified	Unclassified	Unclassified	UL

SECURITY CLASSIFICATION OF THIS PAGE

CLASSIFIED BY:

DECLASSIFY ON:

SECURITY CLASSIFICATION OF THIS PAGE

PREFACE

This Phase II final report describes testing conducted to demonstrate the technical and economic feasibility of a corona-discharge process to decrease the emission of nitrogen oxides (NO_x) from jet engine test cells (JETCs). The work was performed between August 1994 and January 1997. The Air Force Project Officer was Dr. Joseph D. Wander.

EXECUTIVE SUMMARY

A. OBJECTIVE:

The objective of this project was to determine the technical and economic feasibility of applying a gas-phase oxidation process (Pulse-Corona-Induced Plasma; PCIP) initiated by a rapidly pulsed corona discharge as an air pollution control device to the exhaust from jet engine test cells (JETCs). The target pollutant to be treated by the PCIP process was NO_x.

B. BACKGROUND:

A JETC is not a generator of pollutant emissions; however, as an enclosure from which air pollutants are emitted through an identifiable stack, it is subject to regulation under Title 1 of the Clean Air Act (amended 1990). As such, it is also a candidate for imposition of a MACT standard, and the technology selected by EPA as a baseline is not compatible for use on a JETC. Also, as an operation, the JETC is typically one of the largest three or four sources contributing to an installation's emissions, which are regulated under Title 5. An economical emission control system would provide significant relief to the installation in staying in compliance with its permit limits. Conventional emission control technologies for NO_x will not work on JETC exhausts because the control device must accommodate several extreme conditions, including drastic, short-term excursions of temperature; enormous mechanical stresses; and a requirement that resistance to exhaust flow not create a pressure drop across the entire control system of more than 0.5 inches of water. PCIP is one of two technologies that have been able to remove significant quantities of NO_x from combustion exhausts under (small-scale) laboratory conditions equivalent to the JETC environment.

C. SCOPE:

During this study, the PCIP concept developed during the phase I project was refined at bench scale, and improvements to the design were incorporated into a pilot-scale reactor, which also evolved during a program of testing in the laboratory. The final version of the pilot-scale PCIP system was successfully demonstrated on a 300-cfm split of the exhaust from an operational hush house at Nellis AFB, Nevada.

D. METHODOLOGY:

Bench-scale tests were conducted to determine the NO_x removal chemistry and to identify chemical additives which would help scrub NO_x. The subscale PCIP system was designed and built based on these results, and tested at ADA's laboratory to define operating setpoints which were effective for NO_x removal under jet engine exhaust conditions. A laboratory-scale turbojet engine was used to generate the gases for

treatment by the PCIP system. Testing at ADA's laboratory took several months as design modifications were made to improve system performance.

Once removal was obtained in the laboratory using a combination of oxidation by pulse-corona discharge with a spray scrubber, the entire system was moved to Nellis Air Force Base and installed adjacent to a JETC. A 300 cfm slipstream of JETC exhaust was extracted by fan and treated in the PCIP/scrubber system. Differential measurements were made to quantify the performance of the system, including NO_x (conversion and removal), carbon monoxide, hydrocarbons, particulate, temperatures, and flow rates. The results of these tests were used to design and cost a full-scale system capable of treating the exhaust from an entire JETC (up to 4 million cfm).

E. TEST DESCRIPTION:

The bench-scale tests consisted of operating two small-scale (0.5- and 1.0-inch diameter) pulse-corona-discharge reactors while making measurements of the products generated by the corona. Additional laboratory tests included bubbling NO_2-containing gas through various liquid reagents to identify candidate scrubber liquors.

Subscale testing using the bench-scale turbojet engine consisted of optimizing one characteristic at a time. The electrical performance was optimized through testing various electrodes, and both negative and positive polarity. Measurements were made to characterize the electrical performance and power consumption. Pulse-onset voltage was also determined by testing. These electrical variables were set relatively early on in the testing and left at the values that were determined to be effective.

The PCIP system was effective at oxidizing NO to NO_2 and/or other higher oxides. This was determined using a chemiluminescent NO_x analyzer that measured NO separately from total NO_x. Once oxidation was obtained at conditions which duplicated actual JETC conditions, the focus was to design a scrubbing system which would remove the higher oxides of nitrogen. Higher oxides are much more readily scrubbed than NO, and reagents that were identified through literature and verified through earlier laboratory testing were tested in the subscale system. One reagent, sodium thiosulfate, was identified as the best option based on good removal rates and relatively neutral pH. This reagent was used in the balance of testing, including the field tests at Nellis Air Force Base.

A slipstream probe was designed and installed on a JETC at Nellis Air Force Base. Testing at Nellis was conducted over a two-week period. Operating conditions were established for the PCIP/scrubber system at normal JETC operating conditions. Base personnel also set up steady-state conditions to allow ADA to optimize the operation of the PCIP and to make measurements. The data from these tests were used to project the scale and cost for a full-scale system on a similar JETC.

F. RESULTS:

In testing at Nellis Air Force Base, we obtained greater than 50 percent NO_x removal under normal JETC operating conditions. The system for exhaust gas treatment consisted of a slipstream probe, fan, PCIP, and scrubber. The capital cost projections for a full-scale system were based on 50 percent removal of NO_x from 4 million cfm of flue gas at afterburner conditions. The cost of the NO_x removal system is $109,000,000, with operating costs projected for 10 and 50 hours/week operation. The total annualized cost is $14.7 million for 10 hours/wk operation, and $16.8 million for 50 hours/wk. Depending on actual NO_x emission rate assumptions, the cost per ton of NO_x removal ranges from $112,000 to $686,000 for operation in the more normal weekly operation of 10 hours/week. For comparison purposes, NO_x offsets currently cost $1,000/ton.

G. CONCLUSIONS:

The results of this work indicate that cold-plasma-discharge technology is completely practical at much larger scales than are currently being investigated. Specific to the purpose of this project, PCIP in conjunction with wet scrubbing is an engineerable technology for the control of pollutant emissions from large combustion sources that operate on an erratic, low-use schedule. The efficiency of such a PCIP control could significantly exceed the 50-percent goal of this program. At the colossal flow rates generated by JETCs, unit cost to control NO_x is strongly affected by the postreactor scrubbing component. Significant removal of carbonaceous pollutants also occurs, which provides additional compliance benefits and implicitly decreases the life-cycle-balanced cost of control by distributing it over several pollutants. In general, plasma-discharge technologies appear to be technically feasible for a wide spectrum of air-decontamination applications, but the associated costs severely limit their utility.

H. RECOMMENDATIONS:

Application-specific system economics should guide further development of this technology as an emission control for applications to decontamination of combustion exhaust streams. As the trading value of emission credits continues to increase, it is reasonable to expect that both military installations and aircraft-related industries will encounter circumstances in which applying a control to an engine testing facility crosses the economic threshold of practicality. PCIP is also a plausible candidate for treating such high-risk exotics as chemical or biological agents, or rocket propellants, for which the cost of specialized technologies is justifiable.

TABLE OF CONTENTS

LIST OF FIGURES

LIST OF TABLES

SECTION I: INTRODUCTION

A. PROJECT OBJECTIVES

This report describes the Phase II results of a two-phase Small Business Innovation Research (SBIR) program sponsored by the Air Force Research Laboratory, Airbase and Environmental Technology Division (AFRL/MLQE). The Air Force established the goal of developing an efficient NO_x-control strategy for jet engine test cells (JETCs) which does not impact the performance of the jet engines. The overall purpose of this multiphase SBIR program was to evaluate the technical feasibility and cost effectiveness of applying Pulsed-Corona-Induced Plasma (PCIP) to destruction of NO_x.

The objective of Phase I was to demonstrate technical feasibility of using a pulse-induced-plasma-initiated chemical process to control NO_x emissions from the exhaust of a JETC. Phase I was intended as a proof-of-concept program to develop the experimental data required to assess the feasibility of the process. The Phase I program demonstrated that the PCIP process was technically feasible and capable of 90-percent removal of NO_x under simulated jet engine test cell conditions.

The Phase II program was designed to further the development of this technology by developing the data necessary to design a full-scale system and to perform an accurate economic analysis of the technology. This was achieved by scaling up the equipment and demonstrating the technology on a portion of the exhaust from an operational JETC. The sub-scale system tested in Phase II was representative of the geometric configuration of a full-scale module. Laboratory tests addressed issues such as characterizing the wastes.

B. BACKGROUND

The control of acid rain precursors, SO_2 and NO_x, has been the subject of regulations for a number of years. The 1990 Clean Air Act Amendments have specifically targeted significant additional control of nitrogen oxide (NO_x) emissions. Nitrogen oxides are believed to contribute significantly to acid rain, forest and vegetation decline, tropospheric ozone formation, and an increase in the concentration of "greenhouse" gases. NO_x also contributes to visible smog. In response to the concerns related to NO_x, regulators have continued to impose increasingly stringent limitations both for new sources and for existing plants through retrofit control requirements. Industrial stationary sources of NO_x have been required to control emissions by a percentage from baseline by using either modified combustion or back-end removal/control technologies. Each NO_x-control technology is applicable under different process conditions.

JETCs, used by the military and commercial airlines to test-fire new and reworked engines, have been classified by the EPA as stationary sources. Jet exhaust contains nitrogen oxides (NO_x), soot particles, carbon monoxide (CO), and hydrocarbons (HC). The Air Force anticipates that EPA will require at least 50 percent

reduction in total NO_x emissions in the near future. Control of emissions from these facilities represents a very challenging problem because characteristics of the process and of the exhaust gases preclude using any conventional back-end NO_x-control technology such as selective catalytic reduction (SCR) and selective noncatalytic reduction (SNCR). Combustion modifications or front-end emission control are also precluded in a highly tuned process such as a jet engine.

The Air Force has established the goal of developing an efficient NO_x-control strategy for jet engine tests which does not impact the performance of the jet engines. The purpose of this multiphase SBIR program was to meet this Air Force need by developing a cost-effective technology for control of NO_x from JETCs using PCIP destruction of NO_x.

1. JETC Combustion and Byproducts

Jet fuel combustion forms airborne pollutants, including NO_x, hydrocarbons, fine particulate matter, and carbon monoxide. Both gaseous and particulate pollutants are formed from the oxidation of species present in the fuel or in the combustion air.

This SBIR program addressed NO_x, which forms from atmospheric and fuel-bound nitrogen during combustion at the high temperatures present in jet engine combustors. NO_x forms through three mechanisms in any combustion process. Most NO_x emitted from jet engines burning JP-8 fuel is thermal NO_x, formed by oxidation of atmospheric nitrogen. This reaction is rapid at temperatures above 2200 °F. Fuel NO_x, or the oxidation of organically bound nitrogen in the fuel, is the second contributor to jet engine NO_x emissions. This is a smaller contributor since JP-8 contains very little fuel-bound nitrogen. The third source of NO_x emissions is prompt NO_x, which is less well understood, but forms in the flame very quickly. This accounts for slightly higher NO_x emissions than can be theoretically explained when adding the effects of the first two NO_x mechanisms. Air Force jet engine combustors are extremely intense-firing, with high temperatures and high heat release rates. This environment is conducive to rapid formation of NO_x by the thermal mechanism.

The jet engines operated by the Air Force are classified as stationary sources only when operated during brief test periods inside a JETC, which category includes hush houses. JETCs are structures designed to hold jet engines, provide a uniform environment, and suppress noise during static operational tests following maintenance or overhaul. These test facilities are used by the Air Force, Navy, and Army, as well as civilian airline companies and jet engine manufacturers. Although the emissions are emanating from a mobile source (i.e., a jet engine) the courts have ruled that, during these static firing tests, pollutants exiting the stack of the test cell are to be regulated as stationary sources.

There are a variety of designs for JETCs but the most common design incorporates an air-augmentor tube downstream of the engine exhaust to cool the exhaust gases. As the exhaust gases flow into the augmentor tube, ambient air is drawn from outside into the tube to mix with the exhaust gases. In addition to cooling

2

the gases, the augmentor tube dissipates a portion of the kinetic energy of the exhaust blast.

A typical firing of a jet engine in a test cell involves operating the engine at several thrust levels from idle to full load with afterburning. The load on the engine may be held for several seconds to several minutes before proceeding to the next load. There is a prescribed series of operating conditions which each engine is put through to obtain data for an Air Force "acceptance test." Figure 1 shows NO_x emissions as a function time over a typical acceptance test. The engine emissions shown here were measured in the field during our pilot demonstration, and are representative of the F100-PW-100, -220, and -229 engines, which are used on F-15 and F-16 aircraft.
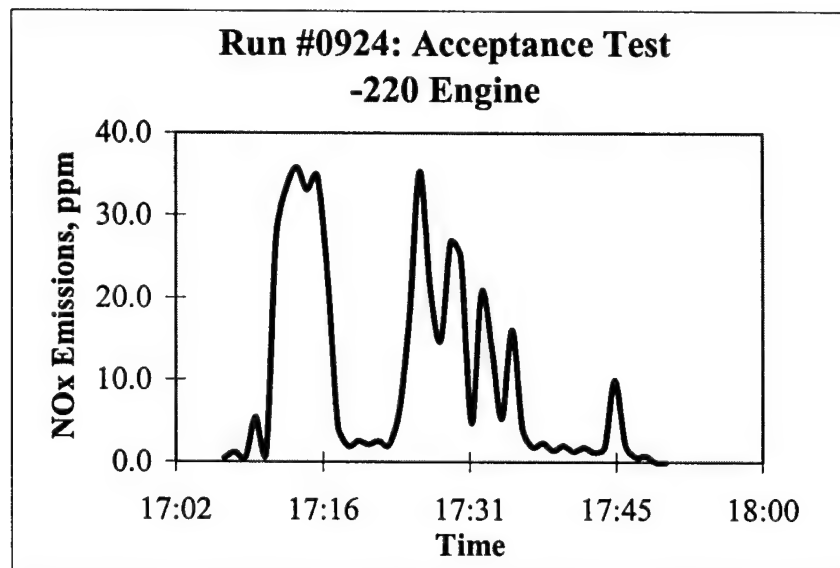
Figure 1: Typical NO$_x$ Emissions During Air Force Acceptance Test

The graph shows only parts per million by volume (ppm$_v$) of NO_x. Table 1 shows typical flow rates for these operating conditions, and the corresponding emission concentrations. The emission measurements show that most of the NO_x is in the form of nitric oxide (NO) and that the total NO_x increases with load from idle to 100 percent. Also shown are emission data for other gas-phase constituents such as CO and total HC. These gases show an inverse relationship with load, until the afterburner is engaged, at which point CO and hydrocarbons are quite variable, and can increase significantly over full-power conditions. This is not surprising since the engines burn up to four times the quantity of fuel in afterburner mode as compared with full military power, for a thrust increase of about 50 percent. The poor burn efficiency associated with afterburner operation explains the increase in CO and HC emissions.

Table 1: Flow Rates and Emissions from Typical JETC

Power Level	Idle	Military	Afterburner
Flow Rate, acfm[a]	~ 200,000	2,100,000	3,721,000
Temperature[a], °F Range		90-154	331-609
NO_x, ppm[c]	4	30-40	30-50
CO, ppm[c]	10-25	<5	70-90

[a]Sorbtech, 1995
[b]Spicer, 1990
[c]ADA Nellis Air Force Base test result

2. Regulatory Perspective on JETCs

EPA-453/R-94-068 (PB95-16237) [*Nitrogen Oxide Emissions and Their Control from Uninstalled Aircraft Engines in Enclosed Test Cells; Joint Report to Congress on the Environmental Protection Agency—Department of Transportation Study*] addresses the Title 1 MACT consideration. In ozone noncompliance areas (and compliance areas, too), emissions from the JETCs are included in the Title 5 permit limits. Permitting a new JETC now generally requires that the installation either decrease its emissions from other sources, acquire emission credits to offset the increased emissions, or combine offsets from decreased emissions and purchased credits to maintain the same net output of each respective pollutant from the installation.

3. Emission Control Approaches for JETCs

Control of emissions from these facilities presents a real challenge because emission is intermittent and because the engine is only minimally tolerant of back pressure (or flow resistance). Other conventional NO_x control technologies are not well-suited to the jet engine test cell application because of the high dilution (low concentration), drastic and condition-dependent temperature gradients, low exhaust temperature, high flow rates, and broad and rapidly changing operating conditions.

Conventional NO_x control technologies are thermal, wet scrubbing, dry scrubbing, or process-based. Several approaches have been evaluated by the Air Force in the past several years in the quest for a cost-effective NO_x control technology.

An overview of Air Force research to control NOx emissions from JETCs (Kimm, Allen and Wander, 1995) summarizes a variety of technologies to achieve this goal. Modifications to the combustor are precluded based on performance impacts or potential physical damage. The Air Force Research Laboratory AFRL/MLQE has sponsored seven independent projects (prior to this nonthermal plasma program) that address exhaust-gas-treatment options. These include exhaust-gas reburning, noncatalytic reduction with additives, metal-based catalytic reduction, photocatalytic decomposition, electrocatalysts, and a solid sorbent bed of magnesium-oxide-coated vermiculite. Each project found the technology to be either technically or economically unfeasible under JETC operating conditions, with the exception of the sorbent bed.

4

AFRL/MLQE is concurrently investigating the use of packed beds of sorbents for use on JETCs (Wander and Nelson, 1993)). Its primary disadvantage is the large pressure drop, for which fans are being used to overcome the flow resistance.

Given the need for a control technology that would be preferable to those already investigated, the Air Force funded this nonthermal plasma development program. The technology seemed well suited to the harsh environment of a JETC due to its fast response time, minimal pressure drop, success with very dilute gas streams, potential to control multiple pollutants simultaneously, and because it can operate in the less-extreme, cooler space behind the augmentor tube.

C. SCOPE/APPROACH

This Phase II SBIR program demonstrated the nonthermal plasma technology on a pilot scale. Initially the work defined the parameters of JETC operation and investigated the products of the PCIP system. Laboratory work at ADA Technologies was directed toward characterizing the chemistry of the process and determining what chemicals could potentially be combined with the PCIP system to promote the NO_x control process.

This laboratory work was incorporated into the design, construction, laboratory testing, modification, and field testing of a subscale PCIP system. The Phase II unit treated a slipstream of exhaust from an Air Force hush house. Ideally, the entire subscale test program would have been conducted on a slipstream from a test cell. However, JETCs are extremely expensive to operate, and are not operated at steady-state conditions for extended periods of time. Therefore, screening tests at ADA's laboratory were a part of the Phase II effort, using a bench-scale jet engine as a surrogate for the test cell.

These initial screening tests were conducted using a bench-scale turbojet engine firing JP-8 fuel. The engine was run at steady-state conditions for long periods to permit making the necessary measurements to characterize the plasma process and make appropriate design changes to the pilot system. These tests provided a base of information that was essential in designing the full-scale system for economic evaluation.

Once sufficient tests were conducted to characterize the process, the subscale system was interfaced to a slipstream of an operating hush house at Nellis Air Force Base. A series of tests were then performed to evaluate the performance of the plasma system under normal JETC operating conditions.

In addition to ADA's NO_x removal measurements, Navy personnel attempted to measure fine particles before and after treatment in the field during testing at Nellis Air Force Base. Oxidation of carbon monoxide and hydrocarbons was also examined. By simultaneously destroying or capturing more than one pollutant, the system could significantly increase its net cost effectiveness.

5

SECTION II: SUMMARY OF NO$_x$ CONTROL TECHNOLOGIES

A. CONVENTIONAL CONTROL OF NO$_x$

Combustion-based NO$_x$-control techniques alter the temperature and air/fuel balance in the primary combustion zone, with associated performance impacts. The performance effects are unacceptable in a highly tuned process such as a jet engine. Earlier efforts to introduce additives to modify the formation of NO$_x$ have also been consistently unsuccessful. Control techniques within the combustor are ruled out on this basis. A number of technologies have been developed for controlling NO$_x$ downstream of the combustion zone. The most prominent and widely applied commercial-scale means of controlling NO$_x$ emissions are selective catalytic reduction (SCR) and selective noncatalytic reduction (SNCR). These techniques rely on reducing nitrogen oxides, as gas species, generally according to the following (ideal) stoichiometry:

$$4NO + 4NH_3 + O_2 \rightarrow 4N_2 + 6H_2O \qquad (1)$$

$$2NO_2 + 4NH_3 + O_2 \rightarrow 3N_2 + 6H_2O \quad (2)$$
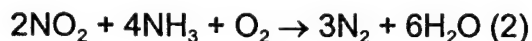
In the SCR system, flue gas passes through a catalyst at temperatures of 600 to 850°F. These catalysts typically contain vanadium, platinum or titanium compounds impregnated on metallic or ceramic substrates. Catalysts made from zeolites are also used for this application and operate at a wider range of temperatures. Innovative variations on SCR technology have taken the form of impregnating catalytically active materials into high-temperature fabric filtration bags (Weber, *et al.,* 1991), placing inserts made of catalysts inside high-temperature fabric filter bags (Wilkinson, *et al.,* 1991), injecting dry catalysts into flue gas (Doyle, *et al.,*1988), and fluid bed adsorbers (U.S. DOE, 1990).

The SNCR process is also called "Thermal DeNO$_x$." Ammonia or urea is injected into the flue gas at temperatures of 1,600 to 2,000 °F to convert NO$_x$ according to reactions (1) and (2). A catalyst is not used in this case, but chemicals can be added to the urea solutions to adjust the temperature window at which the NO$_x$-reduction reactions occur (Epperly, *et al.,*1988).

Several other processes have been developed to lower postcombustion NO$_x$ concentrations without use of ammonia or urea. These processes include reaction with dry calcium hydroxide (Chu and Rochelle, 1989), dry injection of sodium sorbents (Helfritch, *et al.,* 1990), NO$_x$ removal during spray drying (Chan, *et al.,* 1986), a sorbent bed of magnesium oxide (Wander and Nelson, 1993), and reburning (Folsom, *et al.,* 1995).

B. NONTHERMAL PLASMA TECHNOLOGY FOR NO$_x$ CONTROL

The PCIP process uses a cold plasma to destroy NO$_x$ at relatively low temperatures (i.e., < 200 °F). The process involves application of a very sharp-rising,

6

narrow-pulse high voltage to a corona system to produce intense streamer coronas, which bridge across the electrode gap. Streamer corona is the avalanche of electrons generated near a high-voltage wire due to intense gradients in the electric field. Many characteristics of the process make it promising for application to the JETC.

1. Nonthermal Plasmas

Nonequilibrium plasmas produce chemically active radicals that react with pollutant molecules to oxidize or reduce the pollutants to more-benign or -easily collectible forms. The plasma can be generated by discharge reactors or an electron beam. The goal is for electrons in the gas stream to attain a high temperature (high energy), while ion and molecular temperatures remain low. In a plasma system it is only the electrons that can produce chemically active radicals (O, O_2^-, O_2^*, O_3, OH, etc.). The various plasma excitation processes are designed to apply the energy directly to accelerating electrons. This selective heating of electrons is produced by using a very-high-frequency excitation in the MHz and GHz range, or by extremely short pulses of high voltage.

Streamer corona is the avalanche of electrons generated near a high-voltage wire due to intense gradients in the electric field. Research efforts in the late 1970s and early 1980s resulted in the development of the Pulse-Corona-Induced-Plasma Chemical Process (PPCP), which differed from other plasma processes since it could be applied at normal temperature and pressure conditions. This process involves the application of a sharp-rising, narrow-pulse high voltage to a corona system to produce intense streamer coronas, which bridge across the electrode gap. The corona electrode serves as a stable trigger element of streamer corona.

With this process, all the energy is used to accelerate only electrons because the duration of the high electric field is too short to accelerate the ions, which have a much greater mass. The rise in the ion/molecule temperature through electron bombardment is minimized by providing sufficient time between pulses to allow cooling of the ions which have been partially heated through electron collision. The pulse frequency commonly used is in the range of 50 to 500 Hz. This results in a highly nonequilibrium plasma characterized by very high electron temperatures and low ion/molecule temperatures. The PPCP process has been proven to be an effective mechanism for the laboratory-scale treatment of NO_x, SO_2, Hg vapor, volatile organic compounds, odors, and other hazardous and toxic vapors (Masuda 1986 and 1993; Clements 1989; Dinelli 1988).

Testing to date has been performed using laboratory setups and small pilot-scale devices by researchers. These results, when viewed in light of the gas conditions found in JETC exhaust streams, indicate that PPCP offers significant promise for this application.

Masuda found that positive corona was much more effective than negative corona. He concluded that this observation was more a function of the shape of the

corona than the quantity of energy produced. Negative corona forms in individual "tufts" whereas positive corona is more continuous between the wire and the outer cylinder so that the entire reaction chamber can be fully utilized for radical formation.

Keping, *et al.*, (1990) and testing at ADA Technologies has confirmed the finding of Masuda that near-complete destruction of NO_x occurs at very high field strengths and that positive corona was 10 times more effective than negative corona. In addition, Keping presented several key findings regarding NO_x destruction:

- NO_x removal efficiency is inversely proportional to initial NO_x concentration, and greater than 99 percent removal can be obtained at concentrations less than 200 ppm.

- NO_x removal efficiency increases with increased pulse frequency.

Laboratory reactor experiments also demonstrated that NO_x removal was inversely proportional to temperature and that the best NO_x removal occurred at temperatures below 50 °C. This indicates that the system should work satisfactorily in the JETC exhaust, in which temperatures typically remain close to 100 °C.

In addition to NO_x control, research has shown that the PPCP process can also be effective in destroying volatile organic compounds (VOCs) and various chlorofluorocarbons (CFCs). Laboratory tests conducted by Yamamoto, *et al.*, (1990) reported greater-than-99-percent conversion of toluene, 95-percent conversion of methylene chloride, and 67-percent conversion of CFC-113. This suggests that organics in engine exhausts could be controlled by a downstream PPCP system.

2. Features of the Corona Discharge Reactor

The PPCP process is a subset of the corona-discharge-reactor (CDR) technology. CDR can be viewed as a reaction system in which electric energy is delivered to a gas stream to initiate or enhance the rate of beneficial chemical reactions. Such reactors are also referred to as electrical-discharge tubes or reactors in the literature and they have been employed in the past to prepare a variety of chemical compounds at laboratory and small commercial scale. The reaction chemistry in this novel emissions-control approach is thus not in itself new but rather rests on substantial successful applications in systems which have large-scale proof of performance.

a. Systems which Share Similarities with the CDR. Other process systems that are similar to this concept include the electrostatic precipitator (ESP), which is employed to remove particulate matter from flue gas streams, and the ozone generator, which is used to produce chemically-reactive ozone in an air or oxygen feed stream. In practice, the operation of an ESP typically results in both the collection of particulate matter and

8

the generation of varying amounts of ozone, and so the ESP may be viewed as both a particulate emissions control device and a low-efficiency ozonizer.

In the ESP, the electrical operating conditions are controlled to promote charging of particulate matter, which then is attracted to a collector plate of opposite charge for the purpose of removing the particles for either product recovery or environmental control. The precipitator is typically operated under conditions that maximize charging efficiency, and thus collection efficiency, for the particulate matter while simultaneously minimizing sparking or arcing with its subsequent production of ozone. The chemical reactions in an operating ESP are primarily centered around the production of charged or ionized gas species, which then transfer their charge to the entrained particulate matter.

Commercial ozone generators are operated under voltage and current conditions that maximize the net production and highest practical outputs of ozone. In most such systems, production of 2–4 percent ozone with an air feed and of 10 percent or more ozone with an oxygen feed is a typical goal. Thus, the ozone generator is much more a chemical reactor than is the ESP, in which the chemical reactions consist mostly of the *charge transfer* chemistry involved in ion production and charge transfer.

Both ESPs and ozone generators have been developed to the point that both systems are available in scales ranging from laboratory-scale to full-industrial-scale units. In ESPs, this amounts to systems capable of handling hundreds of thousands of cubic feet per minute of flue gas, while in ozone generators, output capacities can be measured in tons per day of ozone in the largest units. However, as mentioned by Masuda (1993), the barrier-discharge design of these ozonators prohibits the high-frequency pulsing required to generate a cold plasma at ambient pressure without overheating.

Whether we compare the ESP or the ozone generator to the proposed CDR, the fundamental similarity resides in the fact that all three systems utilize electrical energy input to promote chemical reactions. The following section examines in more detail some of those reactions and discusses their importance to the goal of removing pollutants from gas streams.

b. Basic Reaction Chemistry in the Corona-Discharge Reactor. Corona-discharge-reactor (CDR) chemistry is based largely on the reaction chemistry of the ions, excited and metastable molecules, and free radicals produced in the corona-discharge region (Glocker, 1939, and Steacie, 1954). Depending on the energy input to the reactor, temperature effects from bulk heating of the gases frequently exert little or no effect on the reaction product suite exiting the CDR.

In generic terms, then, the following simplified reactions represent the types of reactions we can expect in the CDR (Jolly, 1960). In these reactions, (e⁻) refers to electrons derived from the input electrical energy and (M) refers to molecular species present in the gases in the CDR.

a. Electron addition reactions in which negative ions are formed:

$$e^- + M \rightarrow M^-$$

b. Ionization impacts that produce positive ion products:

$$e^-(fast) + M \rightarrow M^+ + 2e^-(slow)$$
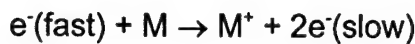
c. Ion clustering reactions that, upon neutralizing impact with electrons, yield new products:

$$M^+ + M \rightarrow (M + M)^+$$

$$(M + M)^+ + e^- \rightarrow Products\ (M_2)$$
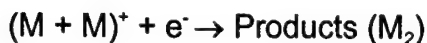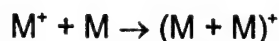
d. Excitation impacts in which metastable, excited-state molecules (M*) are formed and then decay to a lower energy state with the emission of radiation (for example, UV light) or by dissociation into free radicals (for example, formation of hydrogen free radicals from H_2 or hydroxyl radicals from H_2O):

$$e^-(fast) + M \rightarrow M^* + e^-(slow)$$

$$M^* \rightarrow M + light\ emission$$
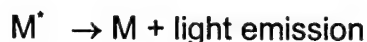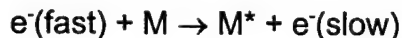
Given the central role played in these reactions by the electrons introduced into the CDR via its high-voltage input, it is not surprising that the final product suite and product yield from a CDR are strongly determined by that input voltage.

Table 2 lists several of the primary variables that will impact the performance of the CDR and that are thus candidates for evaluation in optimizing the operation of the reactor to meet specific goals (in this case, the destruction of NO_x in flue gas).

10

Table 2. Variables Impacting CDR Performance

Applied Voltage	Pressure
Frequency and Duration of Applied Current	Temperature
Electrode/Ground Configuration	Gas Flow Rate
Chamber Size	Gas Composition

SECTION III. BENCH-SCALE TESTING IN PHASE I

A. METHODOLOGY

The objective of the Phase I program was to demonstrate that it is technically feasible to use a pulse-induced plasma chemical process to provide effective control of NO_x from the exhaust of a JETC. The Phase I effort was designed to evaluate several key subsystems of the pulsed-corona-reactor technique. The experimental evaluation was performed at a laboratory scale to determine the advantages, limitations, and operating conditions of the plasma process.

This section describes activities completed during the Phase I program. Proving the practicality of the PPCP required evaluating PPCP against a matrix of critical constraints relating to space limitations, allowable pressure drop, and required NO_x removal efficiency. Phase I was intended as a proof-of-concept program to develop the experimental data required to assess the feasibility of the process.

B. TEST APPARATUS

ADA performed the design and fabrication of experimental equipment to test the PPCP technology in the laboratory under simulated JETC conditions. The laboratory equipment assembled for the Phase I program consisted of four major components :

1. Reaction chambers,
2. Pulsed power supplies,
3. Gas analysis system, and
4. Gas mixing and delivery system.

The experimental phase of the program consisted of three series of tests using both alternating-current (AC) and direct-current (DC) pulsed power supplies.

Laboratory experiments were performed on simulated JETC flue gas. The pulse corona-induced NO_x destruction was evaluated in enclosed stainless-steel reaction cells. Two reaction cells, having diameters of 3 and 6 inches, respectively, were designed and built for these tests. Gas input to the cell was provided by an exhaust-gas-simulation system designed to deliver up to about 10 acfm of mixed gas to the cell. The gas passed through a temperature-controlled water bath/bubbler to introduce H_2O vapor as needed. The humidified mixture was conveyed through heated sample lines to a heater/oven assembly and mixed with the nitric oxide stream, which was metered by a mass-flow controller.

Analyzers were set up and calibrated to perform the laboratory evaluation of the NO_x-removal system. Since part of the destruction process for NO_x involves the oxidation of NO to NO_2, it is necessary to independently measure both of these species during the test program. The ADA Multi-Gas Analyzer was used to directly measure concentrations of nitric oxide (NO), nitrogen dioxide (NO_2), and ozone (O_3) in the laboratory experiments.

12

Three different pulsed power supplies were used. Two of the pulsers were AC-frequency high-voltage generators incorporating Tesla coils with rotating spark gaps. One generator had an adjustable amplitude up to 50 kV, while the second AC generator could supply 250 kV. The third supply was a pulsed-DC corona generator consisting of a conventional automatic voltage controller feeding an oil-filled transformer/rectifier (T/R) set. The high-voltage DC output from the T/R was connected to a bank of charging resistors in series with an adjustable spark gap, which produced the rapid-rising high-voltage pulses.

C. TEST RESULTS

The initial experiments were set up as a series of scoping tests to characterize the reactions and observe general trends that occurred in the corona destruction process for NO_x. The typical trend that was observed is shown in Figure 2. When the power is turned on at low levels, there is an immediate decrease in the concentration of NO. There is also a corresponding increase in NO_2 on almost a 1: 1 basis. This indicates that the first reaction step is the oxidation of NO to NO_2. As the power is further increased, the concentration of NO_2 starts to decrease to a level corresponding to approximately 90-percent removal of total NO_x. No independent power measurements were made on this small, lab-scale test. The rating of the power supply was 30 watts. The scale shown in this figure is a relative power output, to show the trend of increased NO conversion with increased power.
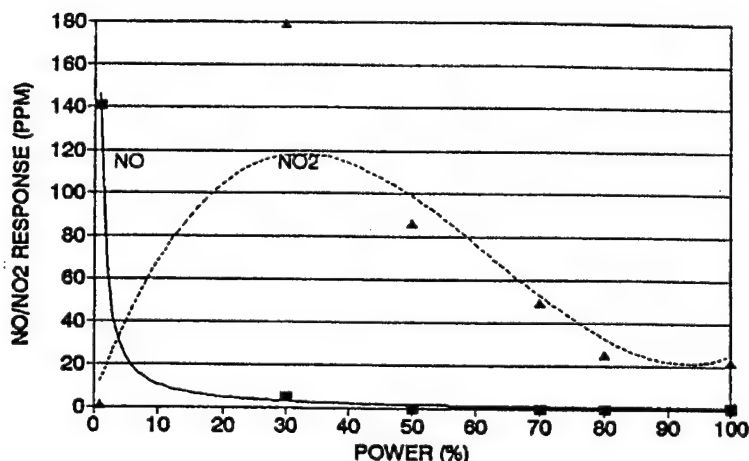
Figure 2: Corona Destruction of NO_x (Durham, 1994)

Additional tests were conducted to evaluate whether the conversion mechanism of NO involves only ozone generated in the cell or whether some direct electrical reactivity of NO is responsible for its conversion and removal. The removal of NO was shown to be a stepwise process in which the NO is first converted into NO_2 and this

species is then further reacted to forms that are not analyzed as NO_x in emissions monitoring protocols. Based on reported conversion chemistry of nitrogen oxides, it was predicted that the predominant final conversion species in damp air is nitric acid. Tests demonstrated that ozone generated during the corona production was the primary oxidizing agent. The presence of OH radicals had a favorable but somewhat minor role in the NO_x destruction.

Since the data proved that the reaction was driven by ozone chemistry, tests were conducted to optimize the production of ozone in the reaction cell. Figure 3 shows results obtained with the pulser and corona electrode optimized. At a temperature of 95° F with 2 percent moisture, it was possible to obtain 60-percent removal of total NO_x at a concentration of 200 ppm. When the concentration was reduced to 100 ppm, the NO_x removal increased to greater than 90 percent. This was very encouraging because the diluted NO_x levels in the exhaust stack of a JETC are well below 100 ppm.
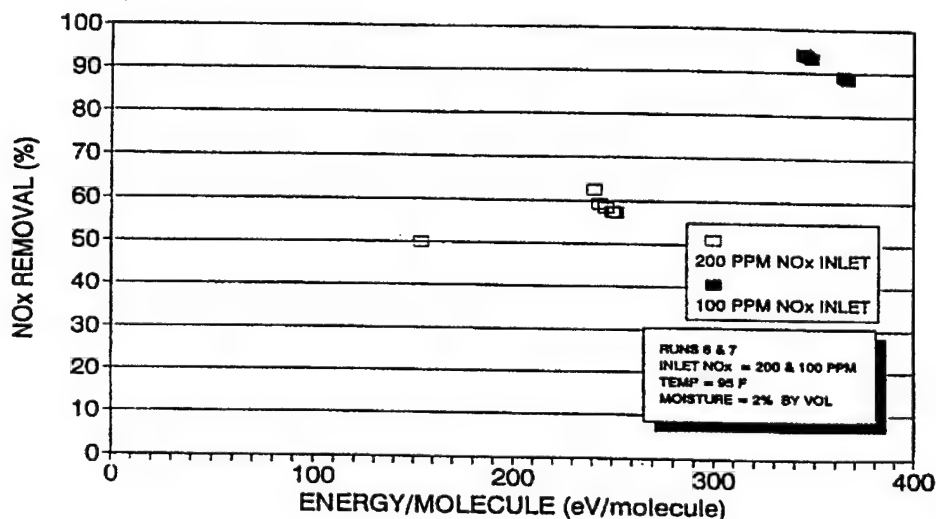
Figure 3: Optimized Pulser Results (Durham, 1994)

D. CONCLUSIONS AND RECOMMENDATIONS FOR SCALE-UP

The Phase I program was very successful as the pulsed-corona plasma reactor demonstrated the capability of NO_x removal levels in excess of 90 percent at simulated JETC conditions. In addition to efficient removal of NO_x, the process has many other features that suggest compatibility with application to the JETC:

- A full-scale corona-plasma-reactor system can be built with a flow-through design resulting in pressure drop less than 0.5 inch H_2O.

- The system can be started up, shut down, and adjusted instantaneously with the operation of the JETC.

- The energization can be increased or decreased to vary the level of NO_x removal.

- Unlike selective catalytic reduction (SCR) and selective non-catalytic reduction (SNCR) processes, efficiency of NO_x removal increases at lower temperatures and lower NO concentrations.

- Other tests have shown that the process is capable of decomposing volatile organic compounds (VOCs) in the gas stream.

- Optimum operating conditions for NO_x removal provides high electric fields capable of charging and collecting soot particles produced by the jet engine.

Because of the low-pressure-drop, fast-response requirements dictated by the operation of the JETC, the electrostatic approach to NO_x control may offer significant advantages over sorbent and catalyst-based processes. Laboratory experiments using a closed reaction cell demonstrated >90 percent conversion of NO to NO_2. These results justified consideration for further evaluation of the process, using a pilot-scale design that represents the geometric configuration typical of a full-scale module.

At the conclusion of Phase I, ADA made recommendations for the scope of a Phase II program to demonstrate the PCIP technology on a pilot scale. The Phase II program was structured to answer many unknowns, including addressing the chemistry of the reaction cell and ensuring that NO_x is scrubbed out and not merely converted into another gaseous pollutant.

SECTION IV. PILOT-SCALE TESTING : PHASE II

A. METHODOLOGY

The Phase II program was designed to further the development of this technology. The overall technical objectives were to determine the capabilities of this technology to control NO_x emissions from a JETC, and to evaluate the costs of a full-scale system. This was accomplished by scaling up the equipment and performing tests of the system on actual JETC exhaust. These tests provided data necessary to design a full-scale commercial system and accurately estimate the costs of the system.

Initially, we obtained data related to the operation of the jet engine test cells. This information was needed to design the test equipment and establish the bench-scale test conditions at ADA's laboratory. We obtained this information by talking with engine manufacturers and JETC operators, and by searching literature for appropriate reference data. This information was essential for constructing a reasonable system which would perform under the harsh and variable conditions of JETC exhaust.

We also performed tests to identify the nitrogen species generated during the pulse-corona destruction of NO_x. We utilized a laboratory-scale corona generator that was capable of operating in either pulse-corona or barrier-discharge mode. ADA's multi-gas analyzer was used with some success to identify gaseous species from the corona region. In addition, we tested scrubbing reagents to determine what chemical composition was required to scrub NO_2 from a gas stream. These were tested in a laboratory-scale bubbler, which allowed us to try several reagents. We were able, through this technique, to identify chemicals that scrubbed NO_2 effectively.

We performed the design, specification, procurement, and construction of the pilot-scale system at ADA's laboratory. Design data were based, in part, on the results of the system requirements and the laboratory chemistry identified for NO_x scrubbing. Critical dimensions for scale-up, such as tube diameter, electrode geometry, electrode spacing, length of treatment zone, and gas velocity, were defined. Additions and modifications for improved performance were made to the system based on the results of testing.

During testing at ADA's laboratory we defined for the pilot-scale system operating parameters that were then applied to the field installation. The bench-scale turbojet engine was used to generate flue gas, which the PCIP system treated. We made measurements using continuous emission-monitoring equipment to determine concentrations of NO and NO_x before and after the corona treatment and after the scrubber, as well as CO and O_2 levels. Many variables were tested during a nine-month test period, including gaseous flow rate, pulser power level, electrode design, spray injection, and inlet NO_x level.

Prior to installation at Nellis Air Force Base, we coordinated with personnel on-site, including a meeting at the site with Nellis Air Force Base personnel and our technical sponsor to define the test conditions and to establish the logistics for

installation of the pilot-scale system. Base access, protocol, and the physical design of the slipstream extraction probe were all of paramount importance in the success of this test program. Success of the field demonstration was based on good communication throughout our time on site.

Once we installed the system on site, the goal was to characterize the performance of the PCIP system on an operating JETC. Although the previous bench-scale tests had demonstrated good performance of the very system that was installed at Nellis Air Force Base, this was not adequate to ensure performance under very harsh actual JETC flue gas conditions. We shipped the system to Nellis Air Force Base, installed the slipstream probe, PCIP, and spray system, and operated the system while jet engine tests were being conducted. Operating parameters that had been established at ADA's laboratory were set, and performance was similar to that seen in the laboratory.

We sampled and characterized the liquid and solid wastes generated from the NO_x control system during the pilot-scale testing. Water samples were analyzed for pH and nitrates to determine a mass balance for the NO_x-scrubbing process. A residue on the interior of the corona region was also analyzed for unburned hydrocarbons.

An economic projection was done to analyze the economics of the PCIP system over a 10-year life expectancy. Design criteria were based on the results of field tests, which produced values for flue gas flow rate (residence time) through a wire-in-tube corona discharge tube, energy required per molecule of pollutant destroyed (eV/molecule), actual removal of NO_x, scrubber requirements, and sizing information. Based on these design data and on power plant equipment (similar scale systems), an economic projection was made for a system to treat a nominal four million cubic feet per minute of flue gas.

B. PILOT-PLANT DESIGN

Figure 4 shows the layout and a photograph of the subscale system as tested at ADA Technologies' laboratory. The system which was field-tested at Nellis Air Force Base is indicated by the boxed area on the figure. Dimensions of the system are shown also.

1. Jet Engines Tested

The engine used for testing in our laboratory was an SR-30 turbine made by Turbine Technologies, Ltd. (Chetek, Wisconsin). This turbine is capable of generating 32 pounds of thrust at a mass flow of 0.84 lb/sec. A single-stage radial compressor feeds a reverse-flow annular combustor can, from which the hot gases expand through an axial-vane turbine. We fired the engine with JP-8 fuel supplied by the Air Force to closely simulate exhaust gas composition from the full-scale engines. This engine provided exhaust gas flow rates that exceeded our requirements, and a slipstream of the exhaust was treated in the CDR. The temperature and composition of the gas were

17
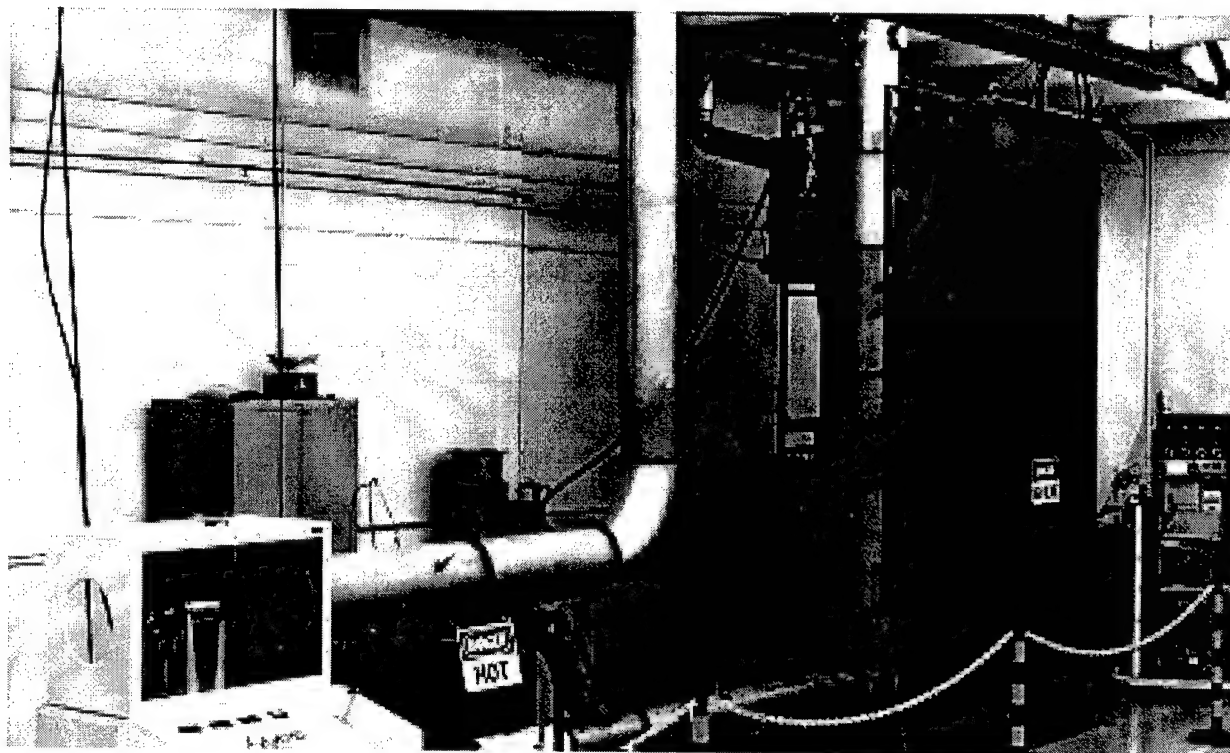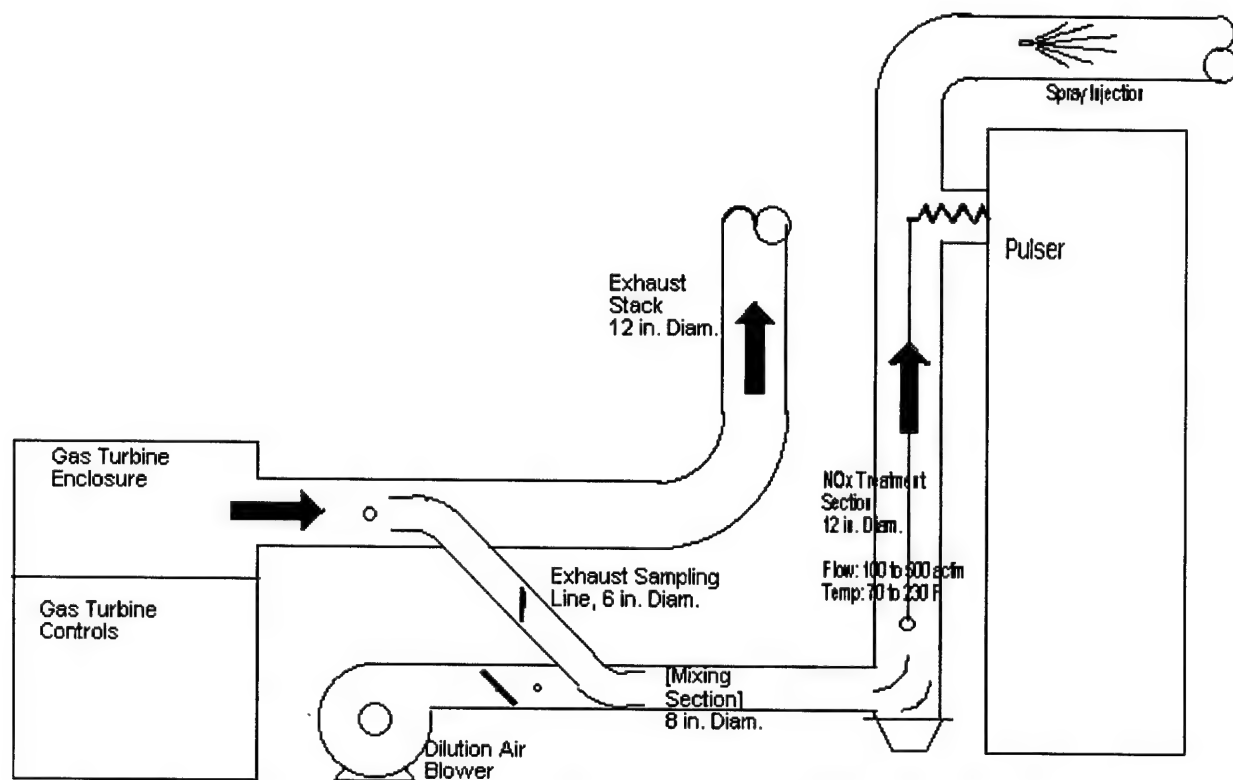
Figure 4: a) PCIP System Design at ADA; b) Photograph in the Laboratory

representative of JETC applications, except that thermal NO_x production was low and hydrocarbons high because of the lower temperatures attained in a small-scale turbine. Nitrogen oxide (NO) was added to the exhaust stream to overcome this and to provide an accurately representative exhaust stream for treatment.

Engines tested at Nellis Air Force Base were Pratt and Whitney F-15 and F-16 engines. There were three engine designs tested: F100-PW-100, -220, and -229. All three are low-bypass, high-pressure-ratio, dual-spool turbofan engines which are similar in design and construction, with the major difference being in the control system. The inlet airflow is approximately 230 lb/sec, and full-load engine speed is approximately 13,000 rpm. Each of these engines has a variable geometry convergent/divergent exhaust nozzle and afterburner, and is typically tested at loads from idle through afterburner operation. The -100 engine has a hydro mechanical unified fuel control (UFC), which requires manual trimming to set operating points, resulting in longer setup and test periods during acceptance tests in the JETC. The -220 and -229 have digital electronic engine control (DEEC), which acquires information from the engine sensors to control automatically at all operating conditions. The emission profiles of these engines were found to be similar, with the maximum NO_x emissions measured during afterburner conditions from the -229.

2. Reaction Cell and Pulsed Power Supply

The schematic of the pulse-corona generator (Figure 5) includes a DC high-voltage (HV) power supply, a pulse generator and a tubular corona-discharge reactor (CDR). A slipstream of the exhaust gas from the jet engine flowed through the CDR, in which the plasma was formed by applying an HV pulse to the corona electrode. The exhaust gas composition, temperature, and flow rate were measured before and after the gas passes through the tube to determine the effects of the plasma. Various currents and voltages were also measured to determine the electrical requirements of the system.

The DC HV power supply was a Hipotronics 220-V AC power supply model 8150-65, which has rated maximum outputs of 150 kV, 65mA, and 10 kW. It consisted of an HV oil-filled tank and a rack-mounted control panel. The oil-filled tank contains all the HV components such as the transformer, capacitors, resistor to measure output voltage, and diode strings, which could be reversed to change output polarity. The control panel contained a motor-driven variable-voltage transformer that controlled the primary voltage on the HV transformer in the tank and, therefore, the HV output to the pulse generator. The power off/on switches, circuit breakers, HV off/on switches, external interlock circuits and other safety features were in the control panel. Also, the DC analog meters in the panel measured the DC HV output voltage (V_{dc}) and current (I_{dc}). The high-voltage resistor, R_V, in the voltage-measuring circuit was actually located in the oil tank. The current-sampling resistor, R_I, was in the ground-return side of the HV circuit. A data logger was connected in parallel with the two analog meters to automatically measure HV output voltage (V_D) and current (I_D). This instrument was of very limited use because of the large transients encountered during HV pulse generation.

19
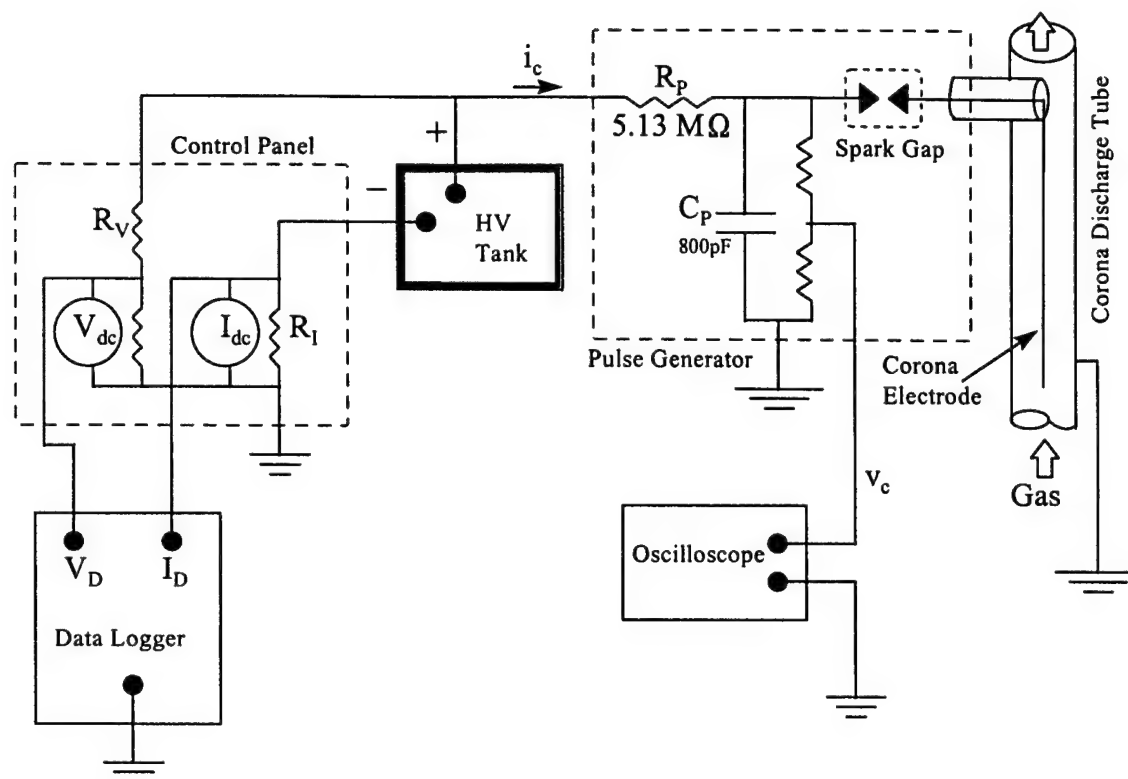
Figure 5: Schematic of Pulse-Corona Reactor

The pulse generator (built by Ion Physics) was 4 feet wide, 5 feet deep and 12 feet high. Although the unit contained essentially three components, it was quite large due to the large spacing required for high voltage in air. The resistor, R_p, in series with the capacitor, C_p, consisted of three 1.71-megaohm resistors in series and it limits the capacitor-charging current, i_c. The capacitor consisted of two 400-pF capacitors in parallel and has a maximum voltage rating of 80 kV. The charging rate for the capacitor could be either increased or decreased by removing or adding resistors or capacitors in appropriate configurations. The spark gap consisted of two movable blocks of carbon enclosed in a Lucite™ chamber filled with a CO_2 atmosphere. The spacing of the carbon blocks was adjusted by an external motor and the spacing determined the voltage at which the spark gap broke down. A voltage divider was connected across the capacitor. The output of the voltage divider was connected to an oscilloscope in an attempt to measure the capacitor voltage waveform v_c. Since the voltage divider was not frequency-compensated, the peak and minimum values of the sawtooth-shaped waveform could only be estimated. However, the pulse period could be determined from the waveform but this period was not constant from pulse to pulse because of variations in the breakdown of the spark gap.

The output of the spark gap was connected to the corona electrode by a 1/4-inch rod through an HV insulator. The corona electrode was centered inside an 11.75-inch-ID steel tube. The tube was carefully grounded to reduce transient signals that occur on all grounds when the spark gap breaks down or there is sparking from corona electrode to tube. The corona electrode extends 7.5 feet along the tube, which determines the active volume for the pulse corona of 5.65 cubic feet. The electrode was centered by the rod through the HV insulator at the top and a Teflon™ bar at the lower end. The corona electrode could be removed and replaced by electrodes of various diameters and surfaces to determine the effects of the electrode on pulse-corona generation. Gas flowed into the bottom of the corona chamber and out the top. The treatment time of the gas was varied by changing gas velocity.

A detailed discussion of the waveforms generated by the system, voltages and currents measured, and the power measurements is included in Appendix A.

3. Laboratory-Scale Plasma and Pilot Scrubber Design

a. Laboratory-Scale Gaseous Chemistry

A laboratory apparatus was assembled to investigate the mechanism and conversion chemistry for NO in a plasma reaction cell. The apparatus is shown in schematic form in Figure 6. There are several features that were incorporated into the apparatus to allow investigation of specific aspects of the reaction process. Valves BV-1 and BV-2 were installed to investigate the effect of ozone on the NO oxidation process. In the default (unenergized) condition, the flow of air mixed with NO passed through the corona cell; when the valves were energized, air passed through the cell to generate ozone, and was then mixed downstream with the NO. This allowed determination of whether ozone and/or other long-lived species were the key component to oxidation of the NO, or if the NO had to be directly exposed to the corona's short-lived radicals for the oxidation to occur. Cells A and B were part of a UV spectrometer instrument that was used to detect and quantify NO_x species in the treated gas stream; ozone also has a distinct UV spectral absorbance that allowed this instrument to measure ozone concentration in the gas stream.

Since the most-desirable end-product of the oxidation was nitric acid, we designed an apparatus to detect nitric acid in the product gas stream. Downstream of the treatment cell, a bed of heated glass beads converted any nitric acid that may be present back into NO and NO_2. The nitric-acid converter was incorporated into the laboratory test setup. This converter consists of Pyrex™ beads at 350–400°C, which have been shown to completely convert nitric acid into NO_2 and NO (Burkhardt et al., 1988). Concentrations of these compounds can be accurately measured using the ADA Multi-Gas Analyzer. We designed a nitric acid calibration source that was used to calibrate the NO_2 and NO response of the ADA Multi-Gas Analyzer to known concentrations of nitric acid processed by the converter. These species were then quantified via UV spectroscopy in Cell B of the apparatus. Valving was installed to allow bypass of the glass bed.

21
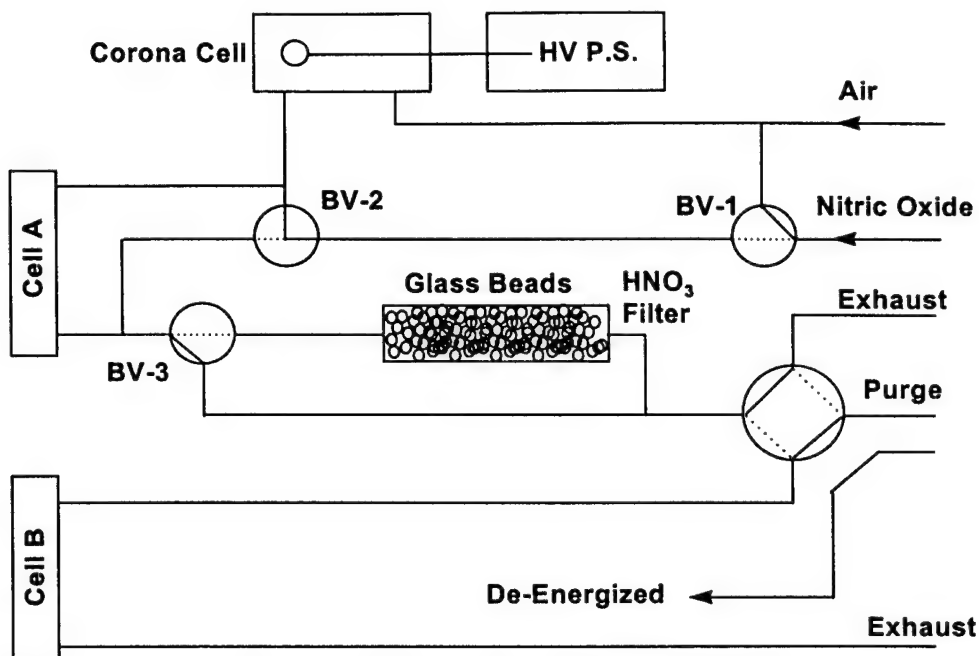
Figure 6: Laboratory Plasma Apparatus

A series of tests was run in this apparatus to investigate the reaction chemistry of the corona-cell NO_x-removal process. Flows of air and certified NO gas mixtures at a known concentration were metered into the apparatus in one of two configurations. In the first mode the flows were mixed upstream of the corona cell and the mixture was then treated by the corona. The treated mixture was passed through the spectrometer cell downstream of the corona cell to determine concentrations of NO, NO_2 and ozone. In the second configuration the air was passed through the corona cell first to generate ozone and the ozone-rich air was then mixed with the NO-laden gas downstream of the corona cell. The initial concentration of ozone in the air was measured in cell A of the spectrometer, and the concentrations of ozone, NO and NO_2 were measured in cell B after reaction of the ozone with the NO gas stream. For some tests the reacted gas stream was passed through the nitric-acid converter and measured with the UV spectrometer equipment associated with cell B. This was done by actuating valve BV-3 and the four-port, two-way valve downstream of the bed.

The UV spectrometer was calibrated to measure NO and NO_2 concentrations. We developed a computational calibration for ozone by using the ozone absorption cross section. We noted that there was evidence of an N_2O_5 peak below 190 nm, this was interpreted qualitatively as an indication of the presence of N_2O_5 in the reaction gas stream. N_2O_5 is an unstable compound, and we were not able to complete an absolute calibration to quantify its concentration with confidence.

The second series of experiments involved measuring the destruction of NO_2 in aqueous solutions of H_2O_2 and other reagents. We were looking for a mechanism to convert NO_2 into nitric acid, and hence scrub the NO_2 from the gas stream. This

solution could be recycled in a full-scale system to reduce the amount of waste scrubber-liquor. In addition, with H_2O_2, no toxic fumes are formed nor are solid waste products generated, such as salts which may foul the process or scrubber liquor removal system.

The laboratory equipment for these tests consisted of metered flow supply lines that dispensed gases into a reagent-filled impinger through a glass frit The gases, which contained known concentrations of NO_2, passed through the reagent bath as fine bubbles. The exhaust from the bath was measured using the chemiluminescent NO_x analyzer to determine NO_2 removal.

To investigate the potential benefits of a silent-discharge plasma for NO_x destruction and to study the effect of corona-cell diameter on NO_x destruction, we fabricated two new reaction cells. One cell was 0.5 inch in diameter and the other 1 inch in diameter. Each cell could be operated as a corona cell or as a silent-discharge plasma by installing a dielectric sheath around the electrode.

b. Pilot-Scale Scrubber Chemistry

The design for the initial pilot-scale test system included the option to inject gases or liquids into the flue gas upstream of the corona-discharge reactor. Since the goal was an economic evaluation of the technology, identifying chemistry that would promote NO_x removal and reduce the power costs associated with the CDR was desirable. Liquid spray prior to the corona was tested and eliminated because of interference with corona generation and inadequate residence time for the spray to distribute through the flue gases. The droplets had a corona quenching effect, reducing the total discharge power. The residence time is short because the droplets, as particles, are precipitated out in the corona-discharge tube.

The final configuration of the spray system, as shown in Figure 4a, included a spray/scrubber downstream from the CDR. This configuration includes mist eliminator material, a high-pressure pump and nozzle injector, and recycling of the spray fluid. Several spray liquor compositions were evaluated based on the results of laboratory tests.

An alternative scrubber configuration was a packed-tower design, which treated a small fraction of the total flow through the CDR. This "scrubber tower" test apparatus bubbled gas through 200 mL of solution. The tower was a 3-inch-diameter, 7-inch-high cylinder. Evaporative cooler pad material was layered in the container to provide extended surface area for contact of liquid with flue gas. The flow rate through the scrubber tower was about three liters per minute, for a residence time of approximately 15 seconds. This configuration was used in all tests marked "scrubber tower," both at ADA's laboratory and in the field at Nellis Air Force Base.

4. Instrumentation for Gas Analysis

The flue gas was sampled at a rate of approximately three liters per minute using a heated sample line to a Baldwin Environmental sample-gas conditioner, which pumps

23

and dries the sample stream. Continuous-emissions-monitoring (CEM) measurements of exhaust-gas composition were made on the dried gas stream using a Thermo Environmental Model 42H NO–NO_x analyzer and a Servomex Xentra 4900 O_2 and CO combined analyzer. During field tests at Nellis Air Force Base, an additional NO_x analyzer, a Thermo Electron Model 10, was used to obtain inlet NO or NO_x measurements (the inlet measurement was time-shared between measuring NO or total NO_x) simultaneously with the outlet measurements.

Type K thermocouples were used throughout the system for temperature measurements. These parameters were logged continuously during the Nellis tests on a Campbell data logger or with a Hotmux™ data collection box (for temperature logging by computer). This continuous logging was essential given the rapid changes in flue gas composition, flow rate, and temperature that the system underwent during on-site tests. Tedlar™-bag samples for hydrocarbons and nuclei particle counter measurements of particle size were collected during selected field tests. The hydrocarbon samples were analyzed by Atmospheric Analysis & Consulting, Inc., laboratory for methane and total nonmethane hydrocarbons by EPA Method 25.1. Pressure drop through the CDR was measured with a Magnehelic pressure gage, and flow rate was determined using standard pitot traverses and cross-checked with a TSI Model 8350 Air Velocity Meter, a thermal anemometer.

C. EQUIPMENT OPERATING PARAMETERS

The variables shown in Table 3 were tested during the laboratory evaluation of the system. Measurements are also shown to indicate how the performance at changing operating conditions was determined. The range of operation for each variable was determined by equipment limitations or by troubleshooting. These variables were selected to characterize the performance of the system under conditions representative of hush houses. The ranges tested did not represent all gas streams or conditions; rather the test program was streamlined towards the specific application.

1. Electrical Variables

The high-voltage pulser and electrode design were modified mechanically during initial system testing. Examples of these changes were positive vs. negative polarity, capacitive load, and charging resistance. Four electrode designs were tested: ¼-inch-diameter coarse-threaded rod, 1/8-inch-diameter smooth rod, ½-inch-diameter smooth rod, and ½-inch-diameter rod with ¾-inch washers spaced 3/8-inch apart along the full length. The ¼-inch coarse-threaded rod was selected as the "best" configuration based on test results, and it was used for the bulk of testing, including all field tests. These variables were optimized relatively soon after testing started, and their settings were determined based on fundamental system performance, such as obtaining at least 60 kV at the spark gap without significant sparkover. The operating ranges for voltage and current supplied to the corona region were optimized over a longer period, based on oxidation of NO, specifically for the flue gas conditions of interest.

2.   NO$_2$ Removal Variables

Operating variables that were used to determine maximum NO$_2$ removal, either in the pulser or in combination with a chemical injectant, are also shown in Table 3. These parameters affected flue gas composition, flow rate, and temperature. They also included injection of gaseous or liquid chemicals, and some testing of solid sorbents. The purpose of these tests was a trial-and-error approach to finding combinations that effectively eliminate NO$_x$ from the gas stream.

3.   Measurements

These parameters were used as our indicators to determine whether performance was good and repeatable. Also values such as pressure drop across the system are design parameters for the full-scale system. RF measurements were made to determine whether radio interference is likely, since JETCs are often adjacent to a flight line. Measurements of flue-gas composition were key to determining overall effectiveness of the system as a whole.

Table 3. Variables and Measurements During PCIP Tests at ADA Technologies

Electrical Variables	NO$_2$ Removal Variables
Corona electrode (four designs tested)	Turbine vs. fan (and load curve on turbine)
DC vs. pulse mode	NH$_3$ injection
Negative and positive polarity	Spray prior to corona discharge
Switch gap varied	Spray post corona reactor
Capacitance	Laboratory tests: bubbler with NO$_2$ or flue gas
Load resistor	
Supply voltage and current (total power)	Methane injection
	Methanol injection prior to corona
	Fan dilution
	Sorbent bed on slipstream of flue gas
Measurements	Residence time
NO, NO$_x$ (and NO$_2$ by difference) : chemiluminescence	Inlet NO
	JP-8 fuel and kerosene
NO$_2$ by Dräger tube	Wet mist eliminator scrubber on slipstream
O$_3$ by Dräger tube	
NH$_3$ by Dräger tube	Temperature
CO, O$_2$, THC	Hydrogen peroxide
ΔP across system, "H$_2$O	Sodium thiosulfate
T$_{corona}$, °F	Sodium hydroxide
Peak pulse voltage (kV)	
Pulse rate (pps)	
RF waves	
Voltage, current supplied to pulser	
Turbine load and operation	
Valve positions	
Spray flow (calculated)	
Pressure drop across scrubber	

26

SECTION V. FLUE GAS TESTING RESULTS AND DISCUSSION

The pilot-scale system was operational beginning in December 1995. Testing began in December and continued through August 1996, when the system was disassembled and shipped to Nellis Air Force Base, near Las Vegas, Nevada. The configuration of the system evolved throughout the testing at ADA, the final configuration being that installed in the field at Nellis in September 1996.

The purpose of testing at ADA's laboratory was to identify both a physical configuration and operating parameter setpoints that successfully removed NO_x from a flue gas that was similar to jet engine test cell exhaust. This was found to be challenging, although technically possible.

The following subsections describe the progress made in each technical area of focus during the testing at ADA's Laboratory.

A. LABORATORY-SCALE TESTING

Since the NO was to be removed from the gas stream, or converted into some more-benign form, it was important to evaluate the details of the process chemistry. To this end, the laboratory test fixture shown in Figure 6 was built to perform PCIP treatment of an NO-doped gas stream, and to analyze the trace gases present at the outlet from the treatment cell. IR spectroscopy and chemiluminescence were used to identify treatment product gas species.

The first series of tests was undertaken to determine the role of the corona in the destruction of NO. The apparatus was run in the two configurations described previously, one in which air was passed through the cell and mixed with the NO gas downstream of the corona, and a second where the entire flow of mixed gases was run through the corona cell. These experiments clearly showed that the long-lived species, such as ozone, participated in the conversion of NO into NO_2. That is, the conversion of a large fraction of the NO was observed for both configurations. Once this was confirmed, additional experiments were run to characterize the reaction of ozone with NO.

The next result was that increased water vapor in the supply air quenched the generation of ozone in the corona cell. A typical result was that air which had been humidified to saturation at ambient temperature (72 °F in the laboratory) showed a decrease in the generation of ozone by a factor of 8, decreasing from 200 ppm in the dry air down to about 27 ppm in the humidified air stream. This result also affected plans to use the bed of heated glass beads for investigation of the presence of nitric acid in the treated gas stream. For nitric acid to form, water vapor must be present in the gas to react with NO_3. However, water vapor quenched the generation of ozone, so that the NO could not be converted into nitric acid in the test apparatus as configured. Further experimentation revealed that the ozone generated in the corona cell was

destroyed in the bed of heated glass beads. Thus the nitric acid analysis testing was abandoned.

A series of experiments was performed to track the oxidation process. Results from a typical experiment are plotted on Figure 7. The UV spectrometer measured 44 ppm of ozone generated in the corona cell; when 78 ppm of NO was mixed with the ozone, an immediate signal for NO_2 was detected. The NO_2 level increased to about 90 ppm, with no spectral evidence of N_2O_5 in the reacted gas. This was interpreted as an indication that the ozone concentration was insufficient to promote further oxidation of the NO_2 to N_2O_5. Further evidence of the validity of the data was presented when the corona was stopped: the NO measurement rose to a steady-state value, and the NO_2 measurement dropped to about 11 ppm.

The negative values shown on the left axis are a result of spectral interference between the ozone and NO_2 signals. When there is excess ozone present, the calculated NO_2 result is negative in proportion to the ozone signal. This is observed twice, at x-axis values of 50 and 225.
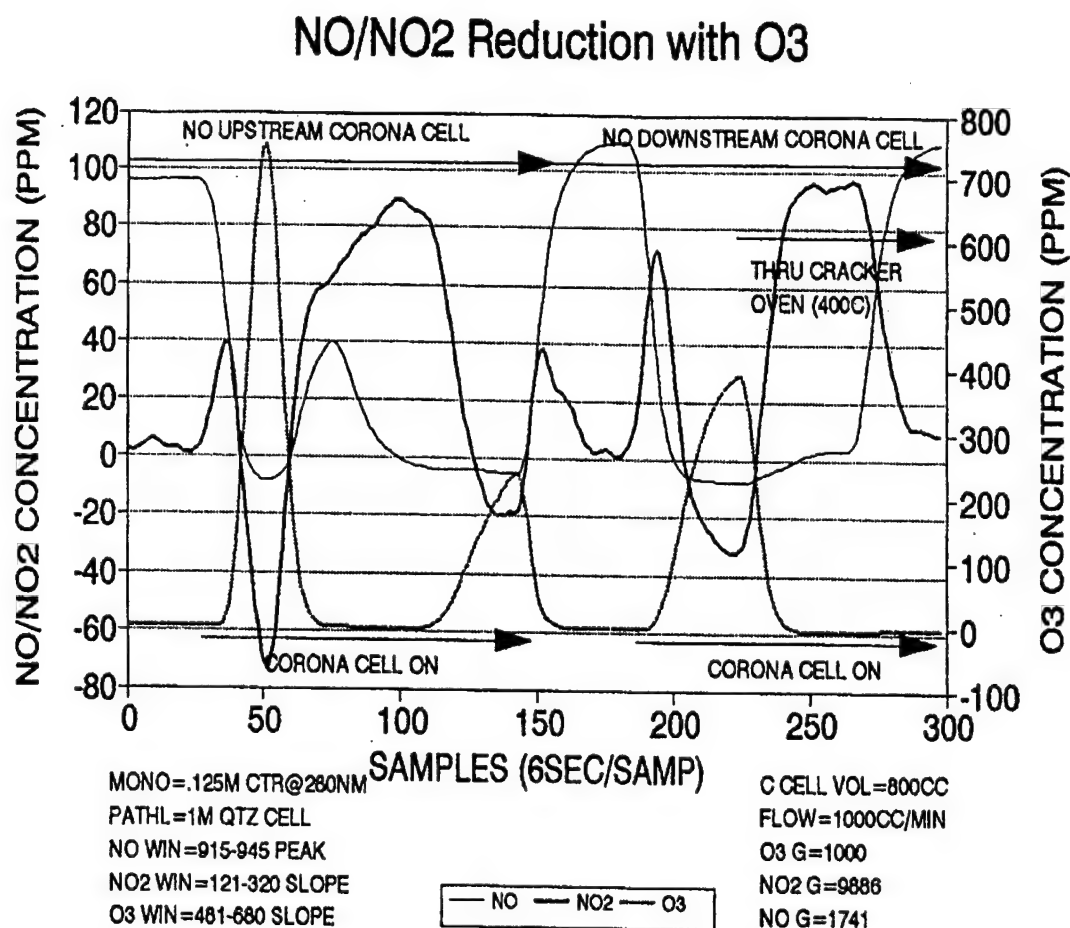
Figure 7: Conversion Test Results

28

Other experiments looked at these species to identify trends. The oxidation of NO into NO_2 by O_3 occurs rapidly. When excess ozone was present, the NO disappeared, and only a trace of NO_2 was detected. We believe this was because the NO was further oxidized to NO_3 and N_2O_5. Although our equipment did not allow us to detect NO_3 in the visible wavelengths with the spectrometer, there was definite evidence of N_2O_5. Because of a lack of information on the spectral cross-section of N_2O_5, it could not be quantified. When the gas stream contained excess NO, the NO_2 level increased because more of the NO was oxidized only to NO_2 rather than further oxidized. Laboratory results showed that the remaining [NO] plus the [NO_2] formed was equal to the initial [NO] concentration, as it should be. According to our experiments a single O_3 molecule is able to destroy 1.5 NO molecules. This ratio was confirmed in a number of experiments with O_3 as the limiting reagent. This result was approximate, but reproducible.

Several experiments were also run with silent-discharge-plasma generators replacing the pulse-corona cell. These experiments showed slight improvement in ozone generation, but the problem of water vapor remained, causing a dramatic decrease in ozone concentration. We then abandoned barrier discharge, since it had no apparent benefits for treatment of this flue gas stream.

Another series of experiments was initiated to evaluate the effect of H_2O_2 as a scrubbing solution for the removal of NO-conversion products from the treated gas stream. In these experiments, we observed a decrease in NO_2 concentration after scrubbing, but the data were thrown into question when the instrumentation indicated negative values of NO_2 after additional gas was bubbled through the scrubbing solution. There was obviously some chemical reaction beyond the oxidation that was changing the response of the UV spectrometer, but we were unable to identify the species involved.

Conclusions for Lab Tests

The first conclusion of the laboratory tests was that the primary mechanism for NO_x destruction in the process was a reaction with relatively stable species, such as ozone, produced in the corona cell. This was demonstrated when similar oxidation rates were measured whether NO was present in the corona cell or mixed in downstream. Also, the addition of water vapor to the gas stream was seen to quench the production of ozone, and thereby prevented experiments to investigate the fate of oxidized species in the treated gas stream.

The pulser converts a small percentage of NO_x into species other than NO_2 or NO_3. This small percentage is seen by our analyzer as a decrease in total NO_x. The chemiluminescent NO_x analyzer measures total oxides of nitrogen, including NO_2 and NO_3, separately from NO. We can see that the pulser converts most of the NO going into it into these higher oxides. Reductive as well as oxidative radicals are present in a corona, so the other species may be N_2O_5, or N_2. There was some evidence that the NO_x destruction was characterized by ozone oxidation of NO to NO_2, then to N_2O_5. No

moisture was present in the flue gas mixture for these tests, the presence of moisture may result in different reaction products, e.g. HNO_3.

In general the laboratory experiments proved disappointing in that they offered partial results that explained some of the NO_x removal chemistry, but ultimately were unsuccessful in providing detailed information on the final products. The laboratory work did, however, provide information on one product by confirming the presence of N_2O_5. It remained for the larger-scale tests on jet-engine exhaust to demonstrate the feasibility of the process.

B. PCIP TESTS AT ADA'S LABORATORY

1. Initial Pilot Pulser Tests: Electrical Optimization

Pilot-scale tests were performed beginning in December 1995. The first step was to configure the pulser, with the assistance of Ion Physics, to generate a corona field in the discharge tube. This involved modifying the resistive load (which was in parallel with the corona load), changing the number of capacitors, and operating the system with the spark gap closed to generate a characteristic VI curve. The final mechanical configuration of the system included 800 pF capacitance, 5.13 MΩ charging resistance, and zero resistive load in parallel with the corona. This configuration was selected based on the ability to attain 60 to 80 kV at the spark gap with an air load through the corona discharge tube. Positive and negative polarity corona were also tested while monitoring NO-to-NO_2 conversion. Positive corona was found to be much more effective than negative polarity, as seen by others (Masuda, 1986, and Keping, 1990). The power supply remained configured with positive corona for the remainder of testing.

Statistical analysis was performed on the results of testing the four electrodes, and the electrode was found to have only a small contribution to the effectiveness of the system at converting NO into NO_2. However, the range of electrical conditions that could be attained without significant sparkover (breakdown in the gas around the electrode) was different for different electrodes. The 1/4-inch-diameter coarse-threaded rod resulted in the best electrical performance, and was installed for the remainder of the testing.

With the configuration as described, it was possible to attain corona-discharge power levels of approximately 350 watts without excessive sparkover. Sparkover was considered acceptable at rates less than one per second. As corona voltage increased beyond this point, the sparking rate would increase, becoming erratic and resulting in decreased corona current. The spark gap was set to the maximum possible gap without excessive sparkover at given flue gas conditions.
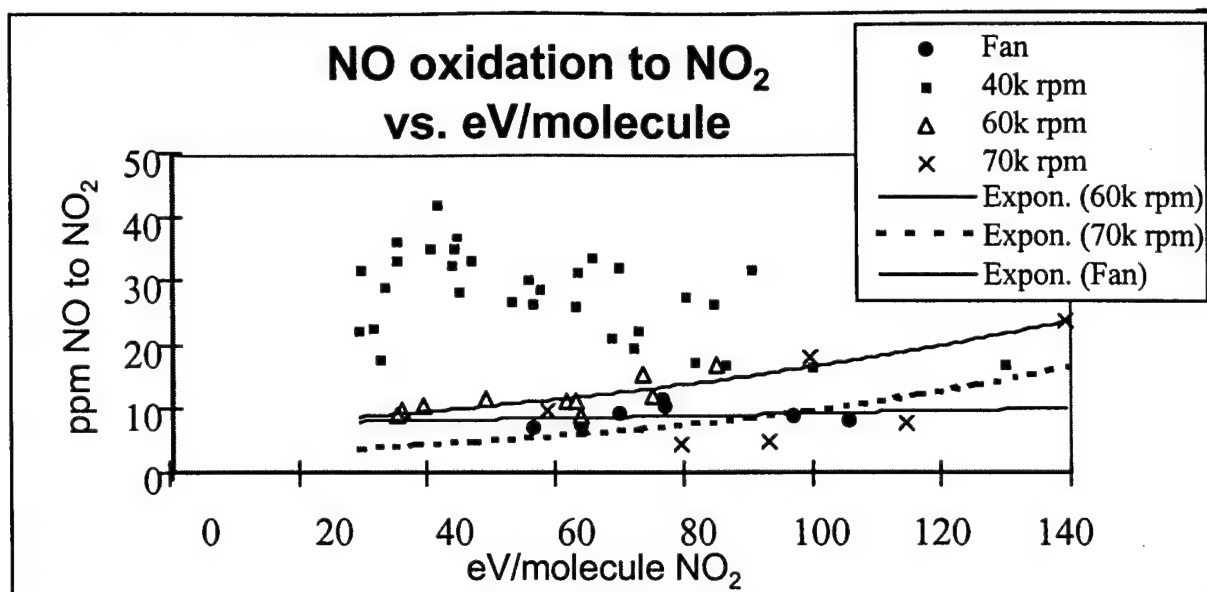
Figure 8. Pilot System Tests: NO-to-NO$_2$ Conversion

Tests were conducted using either turbine flue gas or ambient air (via the fan). The pulser was found to oxidize NO to higher species, with varying effectiveness. For example, tests with ambient air at flow rates of approximately 160 acfm resulted in conversion of about 10 ppm of NO into NO$_2$, even with much higher inlet NO levels (up to 62 ppm). The conversion rate was not strongly dependent on inlet NO concentration or on the energy input to the corona (as measured in eV/molecule, see Figure 8). This appeared to be the maximum conversion attainable, until tests on turbine flue gas were made. Figure 8 shows the NO oxidation measured during early tests, and depicts the dependence on turbine load. Ambient air consistently results in 10 ppm conversion, while tests on turbine flue gas show higher conversion. The maximum turbine load (70 krpm) performance is quite similar to fan-only operation, with the range in data seen here attributable to widely varying residence time in the corona region (0.6 to 4.5 seconds). However, as turbine load drops, the conversion of NO into NO$_2$ for a given energy input (eV/molecule) does improve.

The conversion of NO into NO$_2$ was evaluated through statistical analysis. Variables specified as independent variables were flue gas temperature, inlet NO concentration, turbine load, electrode, HV supply current and voltage, and residence time in the CDR. Oxidation of NO to NO2 was most strongly dependent on turbine load and supply current. The supply current we interpret to correspond to corona-discharge current, which should be the primary driver of NO destruction.

We did not expect to find that the pulser effectiveness was dependent on the turbine load. A search of the literature showed that others have observed a marked improvement of nonthermal plasma discharge systems when hydrocarbons are present in the flue gas (Vogtlin, 1993). Flame Ionization Detector (FID) measurements of our bench-scale turbine flue gas yielded the results shown in Table 4. These hydrocarbon

emissions are higher than those from a full-scale turbine, which is not surprising because residence time is shorter, temperature lower, and mixing probably poorer in a small combustor, resulting in more unburned hydrocarbons in the exhaust at low loads. The hydrocarbon level drops significantly with increased load, as the turbine fires more intensely and temperatures as well as turbulence increase, burning out the fuel more completely. The same trend is seen in CO measurements, shown also in Table 4.

Table 4: Bench-Scale Turbojet Engine Emissions			
	40k rpm	60k rpm	70k rpm
Fuel, lb/hr	19.6	27.4	32.7
O_2, %	20 to 20.7	20 to 20.5	19.5 to 20
CO, ppm	225	120	80
Hydrocarbons, ppm as C_3	250	75	~30
NO_x, ppm	2.0	3.4	4.5
NO_2, ppm	1.6	2.9	4.0

Full-scale turbine emissions data, shown previously in Table 1, show that the values shown for our bench-scale engine are high for CO and hydrocarbons, and low for NO_x. In a number of test runs, we diluted the turbine exhaust gas with ambient air using a fan, in combination with injection of gaseous NO, this generated a flue gas composition more comparable to the full-scale engines. An interesting point to note is that we were unable to duplicate the effect of hydrocarbons in the flue gas by using either methane or propane. The presence of the unburned and reformed JP-8 hydrocarbons was the only successful way to obtain system operation that was characteristic of field operation.

Once the electrical operation of the system was established, as described above, and we had attained the flexibility to convert NO into NO_2 at target NO levels, we began to look at chemical injectants and scrubbing to treat the entire pilot flue gas flow. Scrubbing tests up to this point had been at laboratory scale, and did not treat the actual turbine flue gas but rather simulated flue gas. A project meeting was held at Tyndall Air Force Base in February 1996, which established the goal of eliminating NO_2 either through enhanced scrubber performance or through removal of the NO_2 after it was generated in the pulser.

2. Injectants and Scrubber Systems

The Phase I experimentation resulted in a couple of recommendations for Phase II testing directed at eliminating nitric acid from the gas stream. The first was to install a misting nozzle located at the bottom of the corona reactor to produce water to scrub nitric acid or any precursors. The nitric acid droplets would then be removed by electrostatic processes in the corona-discharge reactor and neutralized with ammonia for disposal. A second recommended test to remove the nitric acid was to inject ammonia into the scrubber. Ammonia rapidly reacts with nitric acid to form particulate

ammonium nitrate. Small amounts of water would be used to wet the tube walls to enhance capture of ammonium nitrate in the ESP. Both of these scenarios would result in the capture of dilute ammonium nitrate solutions.

This subsection describes the results of testing conducted based on these recommendations and other ideas developed during the course of the Phase II program. These tests were typically run with a baseline (inlet) value of 25 ppm NO_x in the flue gas, which is representative of Air Force JETC conditions. The pulser operation was set up to convert about 90 percent (22 ppm) of the NO into NO_2. Several candidate scrubbing techniques demonstrated high removal rates (>80 percent) of NO_x.

Gaseous Injection: Ammonia was injected close to the NO injection point, upstream of the corona-discharge reactor. Ammonia removed NO_x when used in conjunction with the pulser; the disadvantage is that high excess ammonia must be injected, resulting in gaseous ammonia emission equal or greater than the NO_x emission. Results were not acceptable based on this. Storage and handling of ammonia is also a serious issue.

Injection of hydrocarbons into the flue gas did not have major impact on pulser operation nor on effectiveness of conversion of NO into NO_2. The hydrocarbons tested were methane and propane, injected into ambient air (fan operation) rather than turbine flue gases. Concentration ratios of hydrocarbon to NO_x ranged from 2:1 to 8:1.

Liquid Spray Upstream of the CDR: Liquid spray prior to the corona was tested. To maximize the surface area available for gas collection, droplet size must be minimized. Mass transfer between the gas and liquid phases is related to the total volume of liquid holdup per unit volume of spray chamber, and to the Sauter mean diameter (D_s) of the spray droplets. Sauter mean diameter is defined as the total liquid surface area generated inside the absorber divided by the total volume of liquid sprayed. Thus, the smaller the droplets, the greater the area available for mass transfer. Therefore, the generation of a finely atomized spray is desired for the removal of gaseous contaminants by spray scrubbers. When this was tested in our laboratory, we found that the droplets interfered with corona generation and precipitated out quickly in the corona discharge reactor, providing inadequate residence time for the spray to distribute through the flue gases. The inhibition of electrical performance while spraying prior to the corona region prohibited extensive testing of this option.

Liquid Spray Downstream of the CDR: Spray scrubbing is ideally suited to this situation as the rate of transfer is gas-phase mass-transfer limited. This condition exists whenever the liquid-phase resistance can be neglected and the back pressure of the solute over the liquid is small (i.e., nitric acid is highly soluble). A spray scrubber was integrated into the process after the CDR and evaluated. Several dilute scrubber liquor compositions were tested in an attempt to increase the affinity of the nitric acid to enter the liquid phase. Initial tests of this system were not successful. We determined that we needed a sample apparatus that was set up on the actual turbine flue gas and corona products, yet was treating a smaller quantity of the gas. This would enable us to test multiple scrubber solutions quickly, without consuming large quantities of

33

reagent. Therefore, we designed a scrubber tower in the CEMS sampling line which proved to be an effective way of testing the ability of various liquid solutions to remove NO_2 from the flue gas.

The scrubber test apparatus bubbled gas through 100 to 200 mL of solution in the tower. The tower was a 3-inch-diameter, 7-inch-high cylinder that treated 3.5 L/min. of flue gas. Evaporative cooler pad material was placed in the container to provide extended surface area for gas-to-liquid contact. The pressure drop across the tower was measured during several tests and ranged from 8 to 18 inches H_2O. The design is parallel to a "packed tower" design in a full-scale scrubber. We were able to demonstrate success with several different chemical solutions in scrubbing NO_2 using this scrubber tower. The successful chemicals are discussed below.

Sodium Thiosulfate: $Na_2S_2O_3$ at 0.1 molar concentration in water was the most successful chemical solution. It resulted in removal of as much as 80 percent of the NO_x when used in combination with the pulser. The mechanism for scrubbing of NO_2 by sodium thiosulfate is proposed as follows:

$$Na_2S_2O_3 + H_2O \Leftrightarrow 2Na^+ + S_2O_3^{-2}$$

$$S_2O_3^{-2} + NO_2 \Leftrightarrow \frac{1}{2}S_4O_6^{-2} + NO_2^-$$

$$NO_2^- + \frac{1}{2}O_2 \Leftrightarrow NO_3^-$$

In summary,

$$Na_2S_2O_3 + \frac{1}{2}O_2 + NO_2 \rightarrow 2\,Na^+ + \frac{1}{2}S_4O_6^{-2} + NO_3^-$$
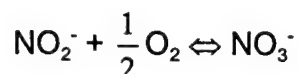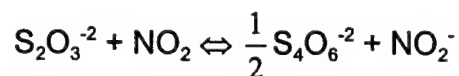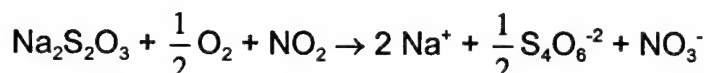
A weaker solution of sodium thiosulfate (0.01 molar) was also tested successfully. This resulted in 75-percent removal of NO_x. The pH of the sodium thiosulfate solutions was close to neutral.

Sodium Hydroxide: NaOH at 0.1 molar was almost as effective at removing NO_x (70- to 75-percent removal was observed). Weaker solutions (0.01 and 0.05 molar) were tested also, resulting in 56- and 64-percent NO_x removal, respectively. The pH of the weakest NaOH solution was above 11.

Hydrogen Peroxide: Three-percent H_2O_2 resulted in greater than 60-percent removal of NO_x.

Based on the success with sodium thiosulfate, which is also the most benign of the successful scrubber liquors, we then improved on the design of the spray injection

system to determine feasibility of designing the full-scale system as a spray tower rather than a packed tower, the benefit being a significantly lower pressure drop.

The laboratory tests using sodium thiosulfate spray into the flue gas showed limited success. The configuration was improved by trying various spray nozzles, spraying counter-current and co-current, providing additional residence time for the spray contact with gas, and incorporating CELdek® [Munters] evaporative cooler material, which is designed to provide excellent gas-to-liquid contact. Under flue-gas operating conditions, which included relatively low flue-gas flow rates and high NO_2 concentrations, the spray removed on the order of 10 percent of the NO_2 from the gas stream. Normal laboratory test conditions, which most closely match a full-scale system, included approximately 25 ppm of NO_x in 300 to 400 acfm flue gas. When flow rates were cut to about a third, and NO_2 concentrations were increased to 34 to 55 ppm, the effect of the spray was confirmed (i.e., 10-percent removal of NO_2). These changes effectively decrease the gas-to-liquid ratio, and demonstrate that, in principle, a spray system should work. Design of a scrubber system, which is already commercially available, was not the focus of this program, but we performed sufficient tests to satisfy ourselves that the technology could be engineered. These tests justified the choice in the full-scale economic evaluation of a spray tower over a packed tower configuration.

Solid Sorbent Bed: A sorbent bed was also tested in the sample line to the CEMS. This was a packed cylinder of material through which flue gas passed prior to measurement by the NO_x analyzer. This experiment successfully removed about 6 ppm (32 percent) of the NO_2 with vermiculite in the sorbent bed. The residence time of the flue gas in the bed was approximately seven seconds. Pressure drop was high through the packed sorbent bed, on the order of 20 inches of H_2O.

C. FIELD TESTING AT NELLIS AIR FORCE BASE

1. Installation and Setup

Preparation for the field testing consisted of communicating plans to Nellis Air Force Base personnel and coordinating with site personnel for support during testing. The program's success was largely dependent on the assistance that Base personnel provided. In August 1996 ADA and AFRC personnel traveled to Nellis Air Force Base to coordinate regarding the details of the September test program. This was essential to the site installation and slipstream probe design, which were based on the information gathered during the site visit. There are two hush houses (JETCs) on Nellis Air Force Base, and at the August meeting our testing was assigned to the west hush house, referred to as Hush House #1. A diagram of the layout of the hush house and ADA's equipment location is shown on Figure 9.
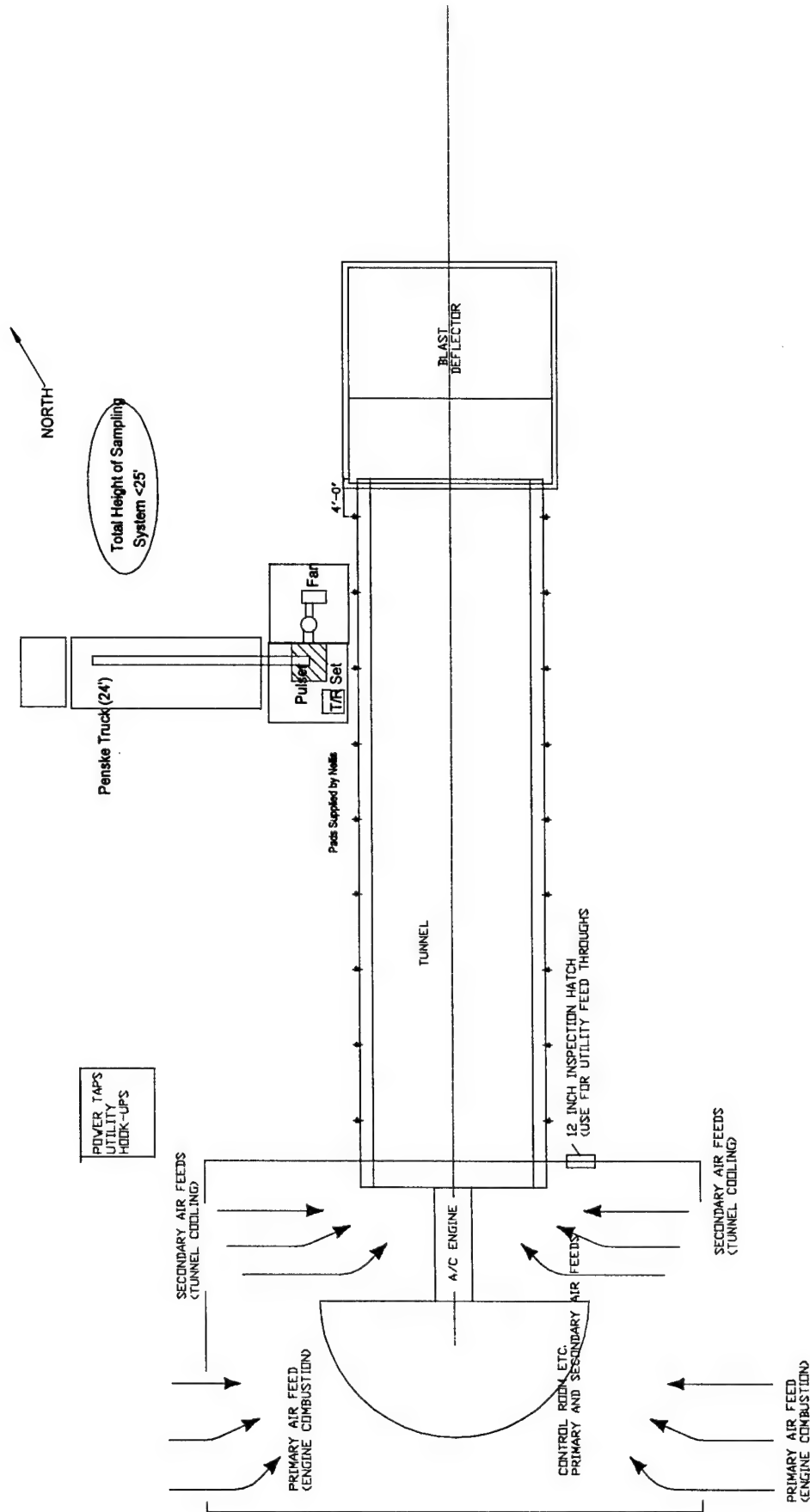
Figure 9: Nellis Air Force Base Hush House and PCIP Layout

NORTH

Total Height of Sampling System <25'

Penske Truck (24')

Fan

Pulse
T/R Set

Pads Supplied by Nellis

BLAST DEFLECTOR

4'-0'

TUNNEL

12 INCH INSPECTION HATCH
(USE FOR UTILITY FEED THROUGHS

POWER TAPS
UTILITY
HOOK-UPS

SECONDARY AIR FEEDS
(TUNNEL COOLING)

A/C ENGINE

SECONDARY AIR FEEDS
(TUNNEL COOLING)

PRIMARY AIR FEED
(ENGINE COMBUSTION)

CONTROL ROOM ETC.
PRIMARY AND SECONDARY AIR FEEDS

PRIMARY AIR FEED
(ENGINE COMBUSTION)

Design and installation of the slipstream probe were the most challenging aspect of the on-site setup. The conditions at the exhaust tunnel include extreme turbulence, temperature swings from ambient to 500° F, very high local velocities in the gas stream, and mechanical vibration from the exhaust tunnel. Since our probe had to be structurally supported by the tunnel itself and by the deflection plate at the end of the tunnel, it had to be able to absorb differential movement between the tunnel and deflection plate. The final design proved to have good structural integrity and some flexibility, allowing the probe to yield somewhat in extremely turbulent flow. Parts were cut and welded in place, and the support included welds to the hush house itself. Welds were inspected frequently over the course of the testing and none was found to have cracked. Upon disassembly, it was noted that bolts in the rear probe support, which were attached to the hush house deflector, had loosened somewhat. In future uses of this probe design, these bolts must also be checked frequently, in addition to the welds. An as-built drawing of the probe is included in Appendix B.

Installation at Nellis began on 9 September. Base personnel had placed level pallets adjacent to Hush House #1 for our equipment, and provided power lines. ADA set up the fan, pulser, corona-discharge tube, transformer, and piping outside. Our truck contained the control equipment for the pulser, as well as instrumentation such as the continuous emissions monitors (CEM) and a computer for logging thermocouple data and for data storage.

The slipstream of flue gas was pulled through five 2-inch-diameter ports in the 4-inch-diameter probe tubing and extracted from the hush house. After passing through the fan, the flow was pushed through the corona discharge pipe. The flue gas then passed through mist-eliminator material to prevent liquid from reaching the corona region, and then through the spray section of ducting, located on the roof of ADA's truck. Measurements made during testing included the parameters shown in Table 5 below. Note that inlet and outlet refer to ADA's PCIP system, inlet being untreated flue gas, and outlet after treatment by the PCIP.

Table 5: Nellis Air Force Base PCIP Test Data

Data	Location(s)	Units	Frequency/Comments
NO and NO_x	PCIP Inlet	ppm	Switch between NO and NO_x each minute
NO and NO_x	PCIP Outlet	ppm	Continuous
CO O_2	PCIP Inlet/Outlet " "	ppm %	Outlet sampled continuously except during brief inlet periods
Particulate matter sizing	PCIP Inlet/Outlet	nm	Grab samples during select tests
Total methane and nonmethane hydrocarbons	PCIP Inlet/Outlet	ppm	Grab samples during select tests
Temperature	East and West Hush House PCIP Inlet and Outlet Ambient	°F	Continuous
Flow rate through PCIP Pressure drop	Several Across PCIP	acfm "H_2O	Measured at various times Once per test
Pulser operation	Control Panel	kV mA	Read manually once per test; continuous log when available
Spray or scrubber operation: composition, quantity		Molar Liters	Each test in which spray or scrubbing was used
Jet Engine operation: Load, rpm, fuel flow	Obtained from operators		Once per test; when available
Ambient conditions: barometric pressure, relative humidity	Base weather station	" Hg %	Daily

2.   Results of Field Tests: On-Site Data

In 10 days of on-site testing, 29 tests were conducted. These tests characterized the flue gas from three engine types, the F100-PW-100, -220, and -229. Testing was conducted during standard hush house operation, called acceptance tests, during troubleshooting of engines, and during periods of extended operation at idle, military, or afterburner loads. These extended periods of operation were requested by ADA and supported by the hush house crew. These extended test periods enabled us to observe the effects of varying some operating conditions of our system such as flow rate, pulser power, and spray injection. Based on these results, we examined NO_2 conversion by the pulser and spray/scrubber effectiveness for NO_2 removal, and we were able to set up good operating conditions during acceptance tests.

A sample of data from one of the final on-site tests is shown in Figure 10. This test run, number 1003C, was during an imitation acceptance test, run at ADA's request. NO_x removal is on the order of 50 percent for this test. Flue-gas flow rate, pulser power, and scrubber liquid composition were set based on previous test results.
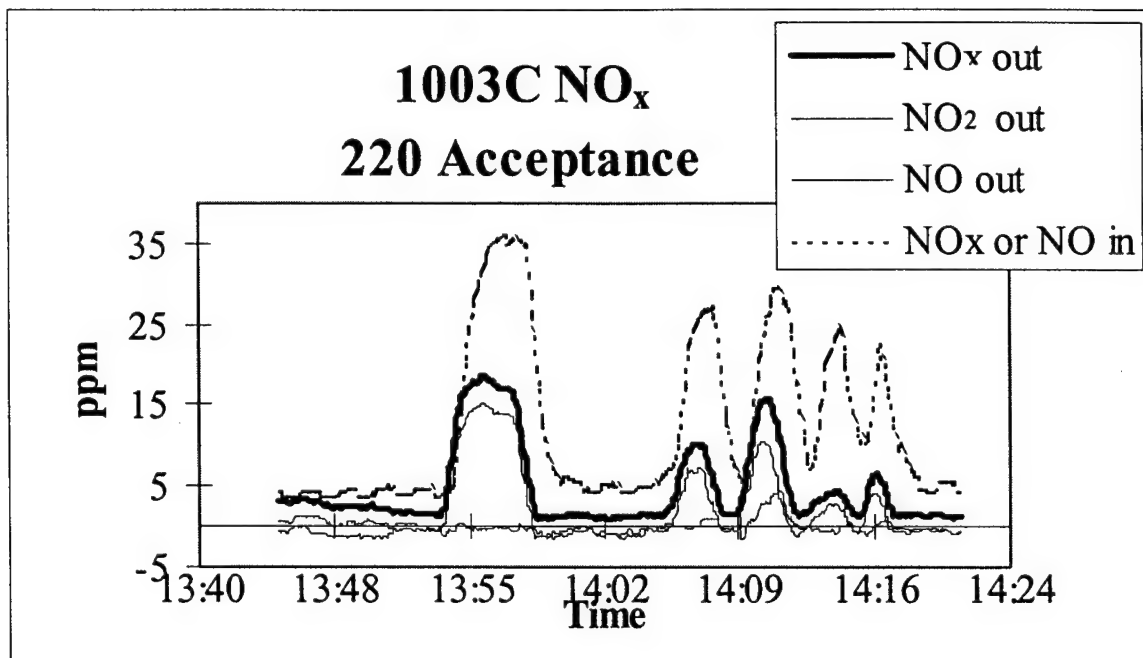
Figure 10: NO_x Removal During F100-PW-220 Acceptance Test

3.   Laboratory Results

Analyses of scrubber solutions for total nitrites and nitrates were performed to confirm that this reaction was occurring. The results from these analyses are shown in Table 6. A sample calculation assuming a balance using the above reactions for test number 1001A/B showed that about half of the scrubbed nitrogen was accounted for as nitrate.

Hydrocarbon test results showed that they are removed in the pulser. Hydrocarbons were measured simultaneously at the pulser inlet and outlet during an engine startup burning "pickling oil," a preservative used in long-term engine storage. These startups are quite smoky, since oil must be burned out of the fuel lines for 30 to 50 seconds. The results of a single Tedlar™ bag pair taken under this condition showed that the CDR system (without scrubber) was removing nonmethane hydrocarbons. Methane in both inlet and outlet samples was 2.1 ppmv, but nonmethane hydrocarbons were 10.3 ppmv at the inlet, and <1 ppmv at the outlet of the CDR. Hydrocarbon bag samples were also taken at steady load conditions on JP-8 fuel. These were taken on two different days, and results varied somewhat. Bags sampled on 30 September indicated that nonmethane hydrocarbons were decreased by the pulser by one to three ppm from inlet levels of two to five ppm. Methane hydrocarbons were again

unchanged. Bags sampled on 2 October, however, indicated that inlet and outlet nonmethane hydrocarbons were consistently 0.5 to 1.0 ppm, not varying with load. Overall, the data indicate that the CDR removes nonmethane hydrocarbons from the exhaust stream. They also indicate that volatile hydrocarbons present in the exhaust are quite low, and vary with operating conditions.

The hydrocarbon results are summarized in Table 7.

Table 6: Laboratory Analyses of Scrubber Solutions

Test Number	Molarity of solution	Result, mg/L Nitrite + Nitrate-N	Spray	Scrubber
0927B	0.1	<0.76	X	
0930B	0.1	4.8	X	
1001A/B	0.01	14.7		X
1001C	0.01	3.9		X
1001C.1	0.1	1.3	X	
1002B	0.1	<0.76	X	
1002B.1	0.01	2.5		X
1003A	0.1	4.5		X
1003C	0.01	3.8		X
1003D	0.1	5.3	X	
1003F	0.01	1.3		X

Table 7 : Hydrocarbon Results

Date	Load/Condition	Inlet ppm		Outlet ppm	
		Methane	TNMHC	Methane	TNMHC
9/27/96	Pickling Oil Startup	1.7	14.1	1.7	8.6
9/30/96	Idle	1.9	3.4	1.9	2.2
	Military	1.5	1.8	1.6	0.6
	Afterburner	1.2	4.8	1.2	2.2
10/2/96	Idle	2.2	0.5	2.2	0.5
	Military	1.9	0.6	1.9	1.0
	Afterburner	1.5	0.6	1.4	0.5
10/4/96	Pickling Oil Startup	2.1	10.3	2.2	0.4

SECTION VI. CONCEPTUAL SYSTEM DESIGN AND ECONOMICS

A. DESIGN USED FOR ECONOMIC ANALYSIS

A flow diagram of the equipment basis for the estimate is shown in Figure 11. It is desired to remove 20 ppm of the NO present in the test cell exhaust, which initially contains 35 ppm. This will be done by oxidizing 25 ppm to NO_2 by means of the pulsed corona reactor and subsequently scrubbing out 20 ppm of the NO_2 (80 percent) with a thiosulfate solution. The gas exiting the scrubber section will thus contain 10 ppm of NO and 5 ppm of NO_2. The captured NO_2 will exit the scrubber as a dilute nitrate salt.
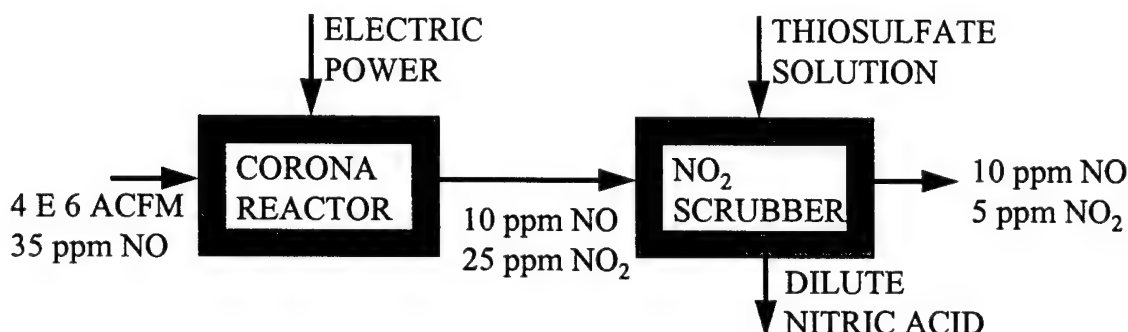
Figure 11 : Flow Diagram for NO_x Removal Process

1. Assumptions

The assumptions used to specify the design of the corona reactor section are shown in Table 8, they include the total flow of 4×10^6 ACFM, a reactor residence time of 1.3 seconds and a reactor height of 30 feet. These values yield a 54-foot x 54-foot vertical bundle of hexagonal tubes, 30 feet in height. Figure 12 gives a rendering of the overall corona reactor–scrubber design. The maximum pressure loss of this design will be at the initial horizontal-to-vertical flow turn and at the upward-to-downward 180-degree flow turn. These losses are estimated to be 0.7 and 1.2 inches of water, respectively, with no turning vanes. The addition of vanes could reduce these pressure losses by more than half.

The energy needed per NO molecule oxidized of 55 eV/molecule and the required oxidation of 20 ppm yields a high-voltage-power requirement of 14 MW. This pulsed high-voltage power can be obtained from 28 individual 500-kW supplies.

A spray tower design for NO_2 scrubbing was chosen over a packed design to minimize pressure drop. To minimize total height and to make use of the corona reactor outside walls, the scrubber will wrap around the corona reactor. A 3-second residence time is sufficient for 80-percent capture of the 25-ppm NO_2 concentration created in the corona-reactor. This residence time and a 30-foot height require a flow area given by a 100-foot x 100-foot footprint minus the 54-foot x 54-foot corona reactor area.   A 10 m$\underline{M}$ solution of of sodium thiosulfate was shown to provide the needed NO_2 capture.

41

To maintain a 5-percent HNO_3 solution, a flow of 10 gpm will be withdrawn. Since thiosulfate will be simultaneously depleted, it will be replaced at a rate of 12 lb/hr.

Table 8. Assumptions for Economic Evaluation

PROCESS ASSUMPTIONS:	4E6 ACFM
	150 DEGREE F
	35 PPM INLET NO
	15 PPM OUTLET NO
	55 eV/MOLECULE NO OXIDIZED
	23 FT/SEC GAS VELOCITY IN CORONA REACTOR - 1.3 SECOND RESIDENT TIME
	10 FT/SEC GAS VELOCITY IN SCRUBBER - 3 SECOND RESIDENT TIME
	L/G = 30 GPM/1000 ACFM
	5% NITRIC ACID WITHDRAWN FROM RECYCLE TANK
	10 M-MOL/L THIOSULFATE CONCENTRATION MAINTAINED
EQUIPMENT ASSUMPTIONS:	30' X 1' HEXAGONAL CORONA TUBES WITH CENTRAL WIRES
	VERTICAL TUBES ARRANGED IN A 54' X 54' PLOT
	(28) - 500-kW PULSED POWER SUPPLIES
	SCRUBBER WRAPS AROUND CORONA REACTOR FOR A TOTAL 100' X 100' PLOT
	SLURRY HOLDING AND RECYCLE TANKS
UNIT COST ASSUMPTIONS:	ELECTRICITY @ $0.05 PER kW-HR
	SODIUM THIOSULFATE @ $0.25 PER POUND
	LABOR @ $30 PER HOUR
	INTEREST RATE @ 10%, 15-YEAR DEPRECIATION

B. ECONOMICS OF CORONA DISCHARGE SYSTEM

The overall annualized cost of the proposed corona reactor depends on both capital cost and operating cost. The yearly cost of the initial capital outlay is added to the annual operating cost for an overall yearly cost. This cost is valid for the present time, since operating and maintenance costs will increase due to inflation, but the present day annualized cost is a good overall picture of the total burden, and line items show the relative magnitude of various cost components.

These costs are given in Table 9. The table shows the assumptions about process and equipment needed to calculate costs. These have been discussed above. The unit cost assumptions list the rates used for raw materials, utilities and labor, as

well as the economic indices used. Based upon these listed assumptions, capital and annualized costs were determined.

The capital cost of the NO_x-control system is broken down into the major component items shown in Figure 12.   These costs were determined from Environmental Elements Corporation (EEC) internal engineering estimates, vendor quotations, and literature citation. The cost of the equipment installation was calculated as a percentage of the equipment costs, based upon previous experience.

The first-year operating and maintenance costs are broken down into utility and raw material costs, based upon the usages described above.   The operating and maintenance labor cost is based upon 20 and 100 hours labor per week for 10 and 50 hours per week operation, respectively.

The capital recovery cost reflects the costs associated with capital recovery over the depreciable life of the system.   This cost is based upon the interest rate and depreciable life given under the unit cost assumptions, as well as the total capital cost.

We see that the annualized cost is mainly composed of capital recovery, which is principally a function of the overall capital cost.   The contributions of yearly operating costs increase the annualized costs from 4 percent to 16 percent, depending on the weekly operating schedule.   The largest cost item is the power supply ($28M), and this cost is dependent upon the energy requirement for the oxidation of NO.

The cost per pound of NO_x removed is shown in Table 10. Since the bulk of the annualized cost is capital, longer operating hours quickly translate into a more-cost-effective system. However, as typical JETC operating periods are an hour or two, 50 hours/week is an unrealistically high number. For comparison, NO_x offset values are on the order of $1,000/ton, or $0.50/lb.

The range shown of costs per pound of NO_x is attributable to different assumptions on the varying operating conditions of JETCs. Both concentration of NO_x and flue-gas flow rate vary enormously, making an integral average difficult to estimate without continuous measurement. For an emission rate of 20 tons NO_x per year, the cost is estimated to be $343/lb NO_x. For the maximum emission rate possible in 10 hours of weekly operation (continual operation at full load, which is not normal JETC operation), the cost drops to $56/lb NO_x. The actual cost for a typical JETC would likely fall between these two estimates.

Table 9: Cost Projections for Full-Scale Corona-Reactor System

CAPITAL ITEM	COST	REFERENCE
CORONA REACTOR EQPMT	$4,500,000	EEC ENGINEERING ESTIMATE
POWER SUPPLIES	$28,000,000	$2/WATT FROM IPC AND IAP
SCRUBBER TOWER	$19,400,000	EPRI CS-3696S[1]
REAGENT PREP/FEED	$6,600,000	"
WASTE HANDLING	$3,600,000	"
INSTALLATION	$47,100,000	R. NEVERIL (1978)
TOTAL CAPITAL COST	**$109,200,000**	

O & M COSTS PER YEAR	10 HR/WK	50 HR/WK
POWER		
Pumps	$114,000	$570,000
Power Supplies	$364,000	$1,820,000
Other	$13,000	$65,000
REAGENT	$1,600	$8,000
OPERATING & MAINTENANCE	$31,000	$155,000
TOTAL O & M YEARLY COST	$523,600	$2,618,000
CAPITAL RECOVERY COST	$14,196,000	$14,196,000
ANNUALIZED COST	$14,719,600	$16,814,000

[1]Shattuck (1984)

Table 10: Summary of Economic Results for Full-Scale System

Equipment Capital Cost	$109,200,000	
Capital Recovery Cost	14,196,000	
Operation Hours per Week	10	50
O&M Yearly Cost	523,600	2,618,000
Annualized Cost	$14,719,600	$16,814,000
$/lb NO_x Removed	$56 to $343	$11 to $69
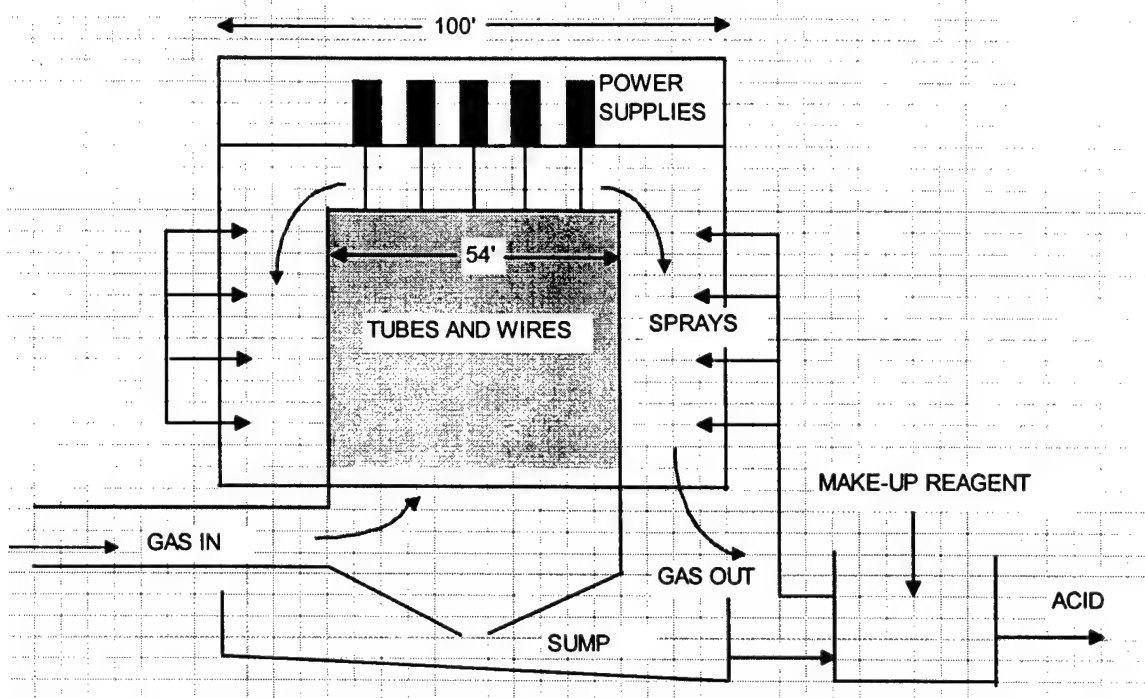
Figure 12 : Two-Stage NO$_x$-Removal Reactor

SECTION VII. CONCLUSIONS AND RECOMMENDATIONS

A. TECHNICAL LESSONS

This program was an extremely successful example of scaling a technology from laboratory-scale (flow rates on the order of liters per minute) to pilot scale (flow rates in the hundreds of cubic feet per minute). Power consumption and NO_x chemistry were both predicted accurately through laboratory testing and verified in the field testing. The following are specific observations that may be useful:

- PCIP is an engineerable oxidation technology and can be used in combination with wet scrubbing for control of pollutants from a source that operates on an erratic, low-use schedule.

- Three reagents were identified as successful scrubbing reagents for NO_2: hydrogen peroxide, sodium hydroxide, and sodium thiosulfate. Of these, sodium thiosulfate was the most effective.

- NO_x control efficiency of the combined system exceeds the project target of 50 percent.

- PCIP simultaneously removes hydrocarbons from flue gas, which also improve oxidation of NO to NO_2.

B. APPLICABILITY OF TECHNOLOGY

- The cost of implementing the combined system is significantly above current NO_x-emission offset prices for the JETC application. Costs of the power supplies and scrubber drive the high capital outlay.

- Treatment of lower-volume, higher-priority toxic emissions may be an application which is more cost-effective than treatment of JETC gases, which emit an extremely dilute and high-volume gas stream.

- As NO_x-emission offset prices increase, it may be worth revisiting the up-to-date costs of capital equipment for control of NO_x from JETCs.

- The high-volume gas stream generated by jet engines results in high capital costs for a secondary control system such as the scrubber train herein. The quantity (number of molecules) of NO to be removed drives the capital cost for power supplies and the cost of power. These two factors (treated gas volume and quantity of pollutant) define the economics for a given application.

REFERENCES

Burkhardt, M., M. Buhr, J. Ray, and D. Stedman, "A Continuous Monitor for Nitric Acid," *Atmospheric Environment*, 22[8], 1575–1578 (1988).

Chan, R., J.L. Casey, K.H. Leong and J.J. Stukel, "Simultaneous Control of Sulfur Dioxide and Nitric Oxide in Spray Dry Scrubbing," 79th Annual Meeting of the Air Pollution Control Association, Paper No. 86-47.7, Minneapolis, Minn. (1986).

Chu, P. and G.T. Rochelle, "Removal of SO_2 and NO_x From Stack Gas by Reaction with Calcium Hydroxide Solids," JAPCA, 39[2] (1989).

Clements, J.S., A. Mizuno, W.C. Finney, and R.H. Davis, "Combined Removal of NO_x and SO_2 from Simulated Flue Gas using Pulsed Streamer Corona," IEEE Trans. on IAS, 25[1], 62-69 (1989).

Department of Energy, "PETC/Industry Partnership: the NOXSO Process," *PETC Review*, U.S. DOE (1990).

Doyle, J.B., E.A. Massitien and W. Downs, "Integrated Injection and Bag Filter House System for SO_x/NO_x/Particulate Control with Reagent/Catalyst Regeneration," U.S. Patent No. 4,793,981, 27 December (1988).

Durham, M.D., D.E. Hyatt, T.G. Ebner, F.J. Sagan, "Application of Pulse-Corona-Induced Plasmas for Control of NO_x from Jet Engine Test Cells," AL/EQ-TR-1994-0020 (1994).

Epperly, W.R., R.G. Broderick, and J.D. Peter–Hoblyn, "Control of Nitrogen Oxides Emissions from Stationary Sources," Annual Meeting of the American Power Conference (1988).

Folsom, B., R. Payne, D. Moyeda, V. Zamansky, J. Golden, "Advanced Reburning with New Process Enhancements," EPRI/EPA 1995 Joint Symposium on Stationary Combustion NO_x Control, Kansas City, Mo. (1995).

Glocker, G. and Lind, S.C., *The Electrochemistry of Gases and Other Dielectrics*, John Wiley and Sons, New York (1939).

Jolly, W.L., *Synthetic Organic Chemistry*, pp. 111–115, Prentice-Hall, Inc., New Jersey (1960).

Keping, Y., L.Ruinian, C.M.Z. Liming, Z. Hong, Z. Hongdi, "Removal of NO_x and SO_2 by Bipolar Corona," The 4th International Conference on Electrostatic Precipitation, 14–17 Sept, Beijing, China (1990).

Kimm, L. T., E.R. Allen, and J.D. Wander, "Control of NOx Emissions from Jet Engine Test Cells," Air & Waste Management Association, 88th Annual Meeting (1995).

Masuda, S. and H. Nakao, "Control of NO by Positive and Negative Pulse Corona Discharges," *IEEE IAS Annual Conf.*, Denver, Colo. (1986).

Masuda, S., S. Hosokawa, X. Tu, Z. Wang, "Novel Plasma Chemical Technologies— PPCP and SPCP for Control of Gaseous Pollutants and Air Toxics," Tenth Particulate

Control Symposium and Fifth International Conference on Electrostatic Precipitation, Washington, D.C. (1993).

Neveril, R.B., J.U. Price, and K.L. Engdahl, "Capital and Operating Costs of Selected Air Pollution Control Systems – V," JAPCA, 28[12] (1978).

Shattuck, D.M., P.A. Ireland, R.J. Keeth, R.R. Mora, R.W. Scheck, J.A. Archambeault, G.R. Rathbun, "Retrofit FGD Cost – Estimating Guidelines," EPRI Research Project 1610-1, Report EPRI CS-3696s (1984).

Steacie, E.W.R., *Atomic and Free Radical Reactions*, 2nd Ed., Reinhold Publishing Corp., pp.32–70, New York (1954).

Vogtlin, G.E., and B.M. Penetrante, "Pulsed Corona Discharge for Removal of NO_x from Flue Gas," in *Nonthermal Plasma Techniques for Pollution Control*, B. M. Penetrante and S.E. Schultheis, eds, Springer–Verlag (1993).

Wander, J.D. and S.G. Nelson, "NO_x Control for Jet Engine Test Cells," AWMA 86th Annual Meeting, Denver, Colo. (1993).

Weber, G.F., D.L. Laudal and S.R. Ness, "Catalytic Fabric Filtration for Simultaneous NO_x and Particulate Removal," EPRI–EPA Ninth Particle Control Symposium, Williamsburg, Va. (1991).

Wilkinson, J.M., P. Chu, K.E. Redinger, T. Gennrich and K.C. Hsieh, "5-MWe SNRB Demonstration Project," EPRI–EPA Ninth Particle Control Symposium, Williamsburg, Va. (1991).

Yamamoto, T., P.A. Lawless, K. Ramanathan, D.S. Ensor, G.H. Ramsey, and N. Plaks, "Application of Corona-Induced Plasma Reactors to Decomposition of Volatile Organic Compounds," 8th Symposium on the Transfer and Utilization of Particulate Control Technology, San Diego, Calif. (1990).

APPENDIX A

WAVEFORMS AND POWER CALCULATIONS

The corona pulse current could not be measured directly because the displacement current flow into the tubular corona chamber is several orders of magnitude larger than the plasma current. However, the approximate average corona power could be calculated from the measured DC and average values of voltage and current.

(a) Capacitor Voltage
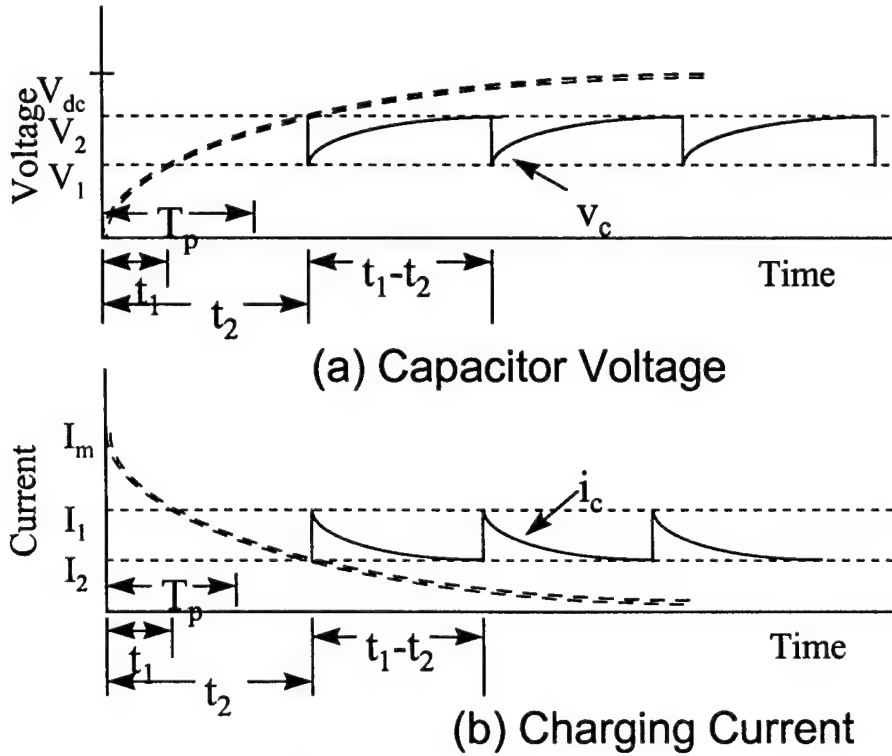
(b) Charging Current

Figure 13 : Waveforms

Calculated waveforms of the capacitor voltage v_c and the charging current i_c are shown in Figure 13. The resistor R_p and capacitor C_p in the spark gap generator determine the shape and period of the waveforms v_c and i_c. When the HV is initially turned on, v_c increases as shown by the dashed line in Figure 13(a) and would approach the applied voltage V_{dc} if spark gap did not break down. Initially i_c has a maximum value of I_m and decreases toward zero as shown by the dashed line in Figure 13(b). This maximum value of current is given by

$$I_m = V_{dc}/R_p \quad \text{amps} \tag{1}$$

49

and the charging time constant is

$$T_p = R_p C_p \quad \text{sec} \tag{2}$$

When v_c reaches V_2, the voltage at which the spark gap was set to break down, C_p discharges through the spark gap and tubular corona chamber. The output of the voltage divider showed when the spark gap breakdown occurred but since it was not frequency compensated, the discharge duration could not be measured. At this time v_c drops to V_1, i_c increases from I_2 to I_1, and the capacitor begins to recharge. Apparently the spark gap stops conducting at V_1 but the various factors that determine this voltage were not analyzed in detail.

The capacitor voltage v_c and charging current i_c can be expressed in terms of V_{dc} and I_{dc} as measured by the two analog meters in the HV control panel.

$$v_c = V_{dc}[1-\exp(-t/T_p)] \quad \text{volts} \qquad t_1 < t < t_2 \tag{3}$$

and

$$i_c = I_m \exp(-t/T_p) \quad \text{amps} \qquad t_1 < t < t_2 \tag{4}$$

where t_1 is the time it takes for the capacitor to charge to V_1 and t_2 the time it takes to reach V_2. Therefore, (t_2-t_1) is the pulse period and the pulse rate, p_r, is given by $1/(t_2-t_1)$. I_{dc} is the average or DC component of the current i_c and can be expressed as

$$I_{dc} = V_{dc}T_p/[R_p(t_2-t_1)][\exp(-t_1/T_p)-\exp(-t_2/T_p)] \quad \text{amps} \tag{5}$$

Equation (5) can be used to determine the validity of calculating the average pulse corona power using the measured values of V_{dc} and I_{dc}.

POWER CALCULATIONS

The approximate average pulse-corona power was calculated neglecting spark gap losses and resistive losses in the ground return between the capacitor C_p and the tubular corona chamber. All of the energy that leaves C_p is assumed to be transferred to the corona pulse. The only loss considered in the pulse generator was the resistive loss in R_p. Therefore, the average output power of the pulse generator, P_{out}, becomes

$$P_{out} = P_{in} - P_r \quad \text{watts} \tag{6}$$

where P_{in} is the average power into the pulse generator from the HV power supply and P_r is the real average power loss in R_p. The HV supply output voltage V_{dc} was

50

assumed to be constant, which is a good approximation except when a spark between corona electrode and tube occurs. The average input power P_{in} can be shown to be

$$P_{in} = V_{dc}I_{dc} \quad \text{watts} \tag{7}$$

The actual power loss P_r in the resistor R_p depends upon $(i_c)^2$, where i_c is given by Equation (4). Using Equation (5) and (7), the real power loss P_r can be expressed as

$$P_r = P_{in}/2[\exp(-t_1/T_p)+\exp(-t_2/T_p)] \quad \text{watts} \tag{8}$$

In all of the power calculations, an approximate average power loss, P_a, in the resistor R_p was calculated using the average value I_{dc} for the charging current:

$$P_a = (I_{dc})^2 R_p \quad \text{watts} \tag{9}$$

Substituting Equation (5) into (9) and combining with (8) shows that the ratio P_r/P_a is

$$\frac{P_r}{P_a} = \frac{(t_2-t_1)\{1+\exp[-(t_2-t_1)/T_p]\}}{2T_p\{1-\exp[-(t_2-t_1)/T_p]\}} \tag{10}$$

This ratio is important because it shows that

$$P_r/P_a \geq 1 \tag{11}$$

for all values of $(t_2-t_1)/T_p$. For example, as $(t_2-t_1)/T_p$ approaches zero, P_r/P_a approaches 1 and as the pulse period approaches infinity the ratio becomes >> 1. Therefore, the approximate average output power of the pulse generator calculated by

$$P_{out} = V_{dc}I_{dc} - I_{dc}^2 R_p \tag{12}$$

is always more than the real power output calculated by Equation (6). This means that the calculated value for the average corona pulse power used in this report is larger than the power actually delivered to the gas due to two reasons: 1) an underestimate of the power loss in R_p and 2) neglecting the power loss in the spark gap. An example calculation is shown below. The equation (12) calculation is used for all power results in this report.

Example Calculation for Power Measurements:

The equations that have been presented describe the general operation of the pulse generator. This can be shown by considering the following typical operating conditions. The resistor and capacitor in the pulse generator were
$R_p = 5.13 \text{ M } \Omega$ and $C_p = 800 \text{ pF}$.
By Equation (2), $T_p = 4.1$ millisecond.

The peak pulse voltage was set to a value where spark-over from corona electrode to tube occasionally occurred. The HV supply voltage was set to produce a maximum value for I_{dc} yet keep the pulse rate about 400 pps or less. Typical values were

V_2 = 67.5 kV, V_{dc} = 90 kV, and V_2-V_1 = 20 kV.

Equation (3) can be used to calculate (t_2-t_1) = 2.6 milliseconds.

Therefore, p_r = 380 pps, and by Equation (5), I_{dc} = 6.1 mA. These values are typical of the recorded values. For these same conditions, the following power calculations were made:

by Equation (7),

$$P_{in} = 548 \text{ watts.}$$

by Equation (8),

$$P_r = 197 \text{ watts}$$

and by Equation (9),

$$P_a = 191 \text{ watts which is only about 3 percent lower}$$

than P_r.

The average pulse corona power as calculated by Equation (12) is

$$P_{out} = 357 \text{ watts.}$$

APPENDIX B

TEST DATA AT NELLIS AFB
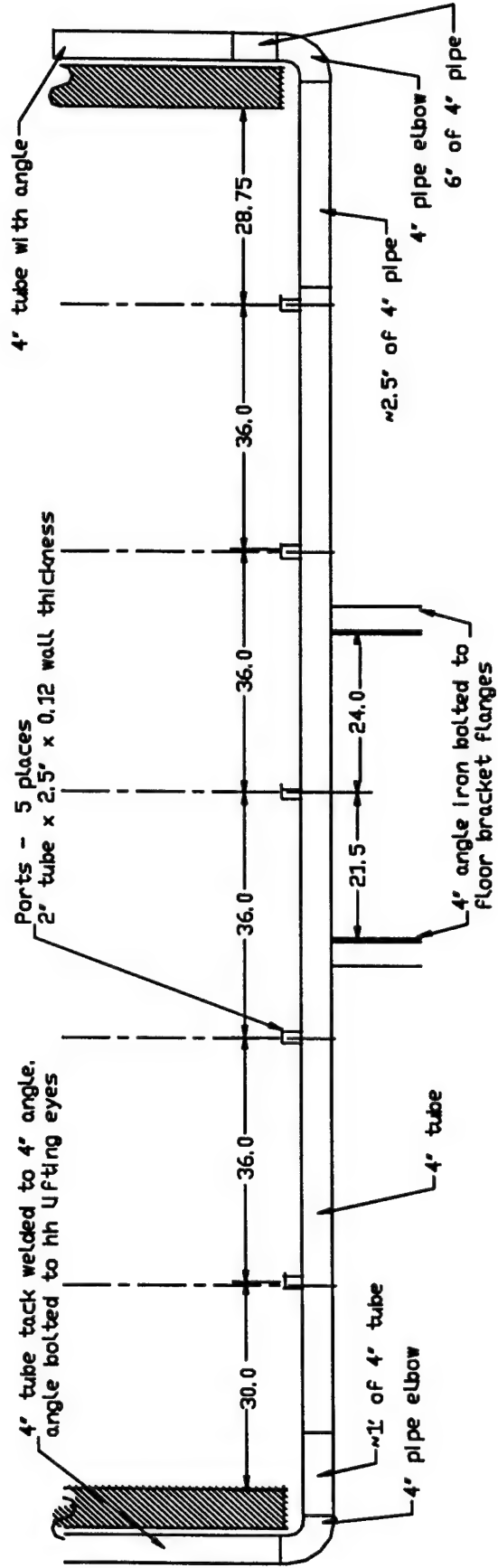
Figure B-1: Probe Installed on Hush House Exhaust Duct at Nellis Air Force Base

54

Table B-1: Test Log for Nellis Air Force Base Hush House NO$_x$ control testing

Test Number	Date Time	Procedure	Engine	Data Obtained	Comments
0923	9/23/96 1717/1835	Acceptance Run; afterburner test	220	NO$_x$, Temperatures: in/ out	Pulser off, partial data.
0924	9/24/96 1707/	Acceptance Run	220	Gaseous in/out, Temps	Pulser on
0925A	9/25/96 1426/1505	Idle for ~15 minutes	100	Campbell/hotmux	
0925B	9/25/96 1606/1700	Military for ~10 minutes	100		
0925C	9/25/96 1744/1754	Afterburner for ~ 10 minutes	100		Spray
0926A	9/26/96 1230/1330	Engine break-in	229		
0926B	9/26/96 1410/15??	Acceptance Run	229		Pulser trips off periodically with vibration
0926C	9/26/96 1610/1651	Idle for ~ 40 minutes	229		
0926D	9/26/96 1752/1815	Military for ~ 20 minutes	229		Spray
0926E	9/26/96 1854/1915	Afterburner for ~10 minutes	229		Pulser off entire run: too much vibration
0927A	9/27/96 0849/0915	Pickled engine: idle for 10-15 minutes	220	HC Tedlar bags; Campbell, Hotmux	
0927B	9/27/96 1014/1117	Military 30 min./idle 5 min./ afterburner 10 min.	220		Spray during Military
0927C	9/27/96 2005/2037	Military ~ 20 min.	220		Increment pulser power

Table B-1: Test Log for Nellis Air Force Base Hush House NO$_x$ control testing, Continued

Test Number	Date Time	Procedure	Engine	Data Obtained	Comments
0930A	9/30/96 0950/1130	Acceptance Run	220	Campbell; Hotmux	Ozone measured after run
0930B	9/30/96 1338/1445	Idle for ~20 min., partial power ~ 10 min., Military ~	220	Campbell; Hotmux; HC Tedlar bags	Spray @ 1434 during Military
0930C	9/30/96 1453/1506	Afterburner	220	Campbell; Hotmux; HC Tedlar bags	
1001A	10/1/96	Acceptance Run	100	Campbell; Hotmux	Scrubber
1001B	10/1/96 1455/1526	Idle ~ 30 min.	100	Campbell (less ch. 2,8); Hotmux	Scrubber
1001C	10/1/96 1710/1819	Military for ~ 30 min., afterburner ~ 10 min.	100	Campbell; Hotmux	Spray and scrubber
1002A	10/2/96 1430/1511	Idle for ~ 30 min.	220	Campbell; CPC w/pulser grounded	
1002B	10/2/96 1635/1800	Idle ~ 15 min., military ~20, afterburner ~15	220	Campbell; Hotmux; HC Tedlar bags; anemometer flow rate	HC at all three loads Spray/scrubber
1003A	10/3/96 0952/1113	Acceptance Run	220	Campbell; Hotmux	Scrubber in CEMS line w/ 0.1 M Na$_2$S$_2$O$_3$; fuel leak shortened run
1003AA	10/3/96 1300/1314	Finish Acceptance Run	220	Campbell; Hotmux	Same as above.
1003B	10/3/96 1314/1344	Idle for ~30 min.	220	Campbell; Hotmux	
1003C	10/3/96 1345/1428	Acceptance Run	220	Campbell; Hotmux	
1003D	10/3/96 1429/1449	Military ~ 20 min.	220	Campbell; Hotmux	Spray

Table B-1: Test Log for Nellis Air Force Base Hush House NO_x control testing, Concluded

Test Number	Date Time	Procedure	Engine	Data Obtained	Comments
1003E	10/3/96 1736/1756	Afterburner ~ ? min.	220	Campbell; Hotmux	
1003F	10/3/96 1756/1818	Acceptance Run	220	Campbell; Hotmux	Scrubber in-line: same one as 1003D
1004	10/4/96 0830/0853	Startup with pickling oil: idle for ~20 minutes	220	Campbell; Hotmux; HC Tedlar bags	

0927A NOx, CO, mA
Pickled 220 Startup / Idle

1004 NOx, CO, O2, mA, kV
220 Idle w/pickling oil

1004 NOx, CO, O2, mA, kV
220 Idle w/pickling oil

0927B NOx, CO, mA
220 Military/Idle/Afterburner

0927C NOx, CO, mA
220 Military

0930A NOx, CO, mA
220 Acceptance Test

Legend: NOx out, NO2, NOx/NO in, mA

y-axis: ppm or mA (0, 10, 20, 30, 40)
x-axis: Time (10:33, 10:48, 11:02, 11:16, 11:31, 11:45, 12:00)

0930B NOx, CO, mA, O2
220 Idle/Partial/Military

Legend: NOx out, NO2 out, CO, NO/NOx in, mA

y-axis: ppm or mA or % (-5, 5, 15, 25, 35, 45, 55)
x-axis: Time (13:26, 13:55, 14:24, 14:52)

0930C NOx, CO, O2, mA
220 Afterburner

Legend: NOx out, NO2 out, CO, NOx/NO in, mA

y-axis: ppm, mA, or % (-20, 0, 20, 40, 60, 80)
x-axis: Time (14:52, 15:00, 15:07, 15:14, 15:21)

1001A NOx, CO, mA
100 Acceptance Test

NOx out
NO2 out
NO/NOx in
mA

1001B NOx, CO, mA
100 Idle

NOx out
NO out
CO
NO/NOx in
mA

1001C NOx, mA
100 at Military/Idle/Afterburner

NOx out
NO out
NO/NOx in
mA

1002A NOx, mA
220 Acceptance/Idle

1002A Calibrations

1002B NOx, mA
220 Idle, Military, Afterburner

1003A NOx, mA
220 Acceptance Test

1003AA NOx, CO, mA
220 Acceptance, Cont'd

1003B NOx, CO, mA
220 Idle

**1003C NOx
220 Acceptance**

Legend: NOx out, NO2 out, NO out, NOx in

**1003D NOx, CO, mA
220 Military**

Legend: NOx out, NO2 out, CO, NOx in, mA

**1003E NOx, mA
220 Afterburner**

Legend: NOx out, NO2 out, NO out, NO/NOx in, mA

1003F corrected data

1004 NOx, CO, O2, mA, kV
220 Idle w/pickling oil

0923 NOx in and out: pulser off

0923: NOx inlet and outlet, calibration corrected

0923 Temperatures: 220 Acceptance Run

0924 Inlet and Outlet NOx, Calibration Corrected

0925A CO, NOx, mA
220 Idle

0925B NOx and mA
220 Military: pulser on

0925C NOx, CO, mA
220 Afterburner

68

0926A NOx, CO, mA
229 breakin/acceptance

0926B NOx, CO, mA
229 Acceptance Run

0926B NOx, CO, mA
229 Acceptance Run

ADA Technologies

3/3/97

0926C NOx, CO, mA data
229 Idle

0926D NOx, CO, O2
229 Military

Cal corrected NOx in and out; Pulser off
0926E 229 AB